High-Resolution Seismic Reflection Profiling and Modeling of Hydrogeologic System, Goddard2 Well, Northwest Boise, Idaho

Report Prepared for Grant 684-K102 to Idaho Water Resources Research Institute, University of Idaho, Moscow, Idaho 83843

Warren Barrash
Martin E. Dougherty

Center for Geophysical Investigation of the Shallow Subsurface
Boise State University
Boise, Idaho 83725

Technical Report BSU CGISS 95-17
December 1995

TABLE OF CONTENTS

	Page
Abstract	1
Introduction	2
Hydrogeologic Setting	3
High-Resolution Shallow Seismic Reflection Profile	3
Seismic Data Acquisition	4
Near Surface Environment	4
Noise Tests	4
Seismic Reflection Lines	5
Results	5
Stratigraphic Interpretation	5
Unit 1: Acoustic Basement	6
Unit 2: Prodelta/Deep-Water Environments	6
Unit 3: Delta-Plain Sand	7
Unit 4: Floodplain/Delta?	7
Structural Interpretation	7
Conceptual Model	8
Analysis of Pumping Tests	10
Well Losses	10
Step Test	11
Constant-Rate Test	12
Engineering Estimate of Transmissivity	12
Evaluation of Non-Leaky Aquifer Model	12
Numerical Model	13
Modeling Non-Symmetric Flow to a Well with MODFLOW	13
Model Configuration	14
Sensitivity Analysis	16
Summary	16
Recommendations	17
Acknowledgments	18
References Cited	19
Tables	22
Figures	30
Appendix A. Modeling Axially Symmetric and Non-Symmetric Flow to a Well with MODFLOW	A1
Appendix Tables	A9
Appendix Figures	A11

LIST OF TEXT FIGURES (continued)

Figure		Page
7A	CGISS high-resolution seismic reflection profile	36
7B	Seismic stratigraphic units and faults interpreted from CGISS seismic line	37
8	Schematc diagram of floodplain environment, after Walker and Cant, 1979	38
9	Lithologic logs of deep wells, including Goddard1 well, located along an orientation parallel to likely direction of sediment influx	39
10	Lithologic logs of deep wells, including Goddard1 well, located along an orientation at a high angle to likely direction of sediment influx	40
11	Well construction and lithologic logs for wells monitored during the Goddard2 pumping test	41
12	A. Semilog plot of drawdown vs time for step drawdown test B. Step drawdown data show constant trend indicating minimal non-linear well loss	42
13	Log-log plot of drawdown vs time using Theis conceptual model	43
14	Discretization scheme in MODFLOW	44
15	Schematic diagram of hydrologic system modeled for Goddard2 well pumping test	45
16	Section through hydrostratigraphic units and the partially penetrating pumping well	46
17	Log-log drawdown vs time plot for constant-rate pumping test at the Goddard2 well	47

LIST OF APPENDIX TABLES

Table		Page
A1	Numerical model characteristics	A9
A2	SIP input values for all MODFLOW and RADMOD runs	A10

LIST OF APPENDIX FIGURES

Figure		Page
A1	Discretization scheme	A11
A2	Well geometry, grid geometry and drawdown at the well	A12
A3	Scenario 1 - Theis conditions	A13
A4	Comparison of model results at the pumping well for Scenario 1	A14
A5	Scenario 2 - Hantush Case 2 conditions	A15
A6	Comparison of model results at the pumping well for Scenario 2	A16
A7	Scenario 3 - Partially penetrating pumping well in a confined, anisotropic aquifer	A17
A8	Comparison of model results at the pumping well for Scenario 3	A18
A9A	Scenario 4 - Intersecting no-flow boundaries. Relative positions of wells (real pumping well and image wells) and no-flow boundaries	A19
A9B	Scenario 4 - Intersecting no-flow boundaries. Relative positions of wells (real pumping well, observation well and image wells) and no-flow boundaries	A20
A10A	Comparison of model results at the pumping well	A21
A10B	Comparison of model results at an observation well	A22

HIGH-RESOLUTION SEISMIC REFLECTION PROFILING AND MODELING OF HYDROGEOLOGIC SYSTEM, GODDARD2 WELL, NORTHWEST BOISE, IDAHO

Warren Barrash and Martin E. Dougherty
Center for Geophysical Investigation of the Shallow Subsurface
Boise State University, Boise, Idaho 83725

ABSTRACT

The western Snake River Plain is filled, in its upper part, with sediments deposited in a variety of lacustrine and associated subaerial environments. This study examines the usefulness of high-resolution seismic reflection profiling for identifying sedimentary environments and geologic structures in the western Snake River Plain at depths that have significance for hydrologic behavior at individual wells and for the ground-water flow system in general. In addition, this study applies a discretization scheme in MODFLOW developed to accurately model single-well pumping tests which are common, by design or default, in the lower Boise River valley. A study area was chosen in northwest Boise where only the pumping well (Goddard2 well) responded during an 8 hr test and the well exhibited negative boundary effects, and where available subsurface data from wells were not sufficient to develop a conceptual model for analysis of the Goddard2 well.

A high-resolution seismic reflection line was run by the Boise State University Center for Geophysical Investigation of the Shallow Subsurface (CGISS) at the Western Idaho Fairgrounds across the surface projection of the Eagle-West Boise fault. This line provided an image of sedimentary environments and geologic structures between about 150 ft (45 m) below land surface (BLS) and about 2300 ft (700 m) BLS. This region of imaging includes the depth intervals used for municipal and industrial water supplies, and overlaps with deep seismic lines which image at depths starting about 1000 ft (300 m) BLS.

Four units representing different rock types and/or sedimentary environments are interpreted from the CGISS seismic line as, from older to younger: unit 1, volcanics; unit 2, prodelta/deep-water lacustrine environments; unit 3, delta-plain sand; unit 4, floodplain/delta? environments. Down-to-basin faulting offsets older units more than younger units. A few faults (such as the Eagle-West Boise fault) accommodate significantly greater offset than others. Projection of units and structural trends southwestward from the CGISS line to the Goddard2 well suggests that the Goddard2 well is completed in a sand stringer in a floodplain environment.

Engineering analysis of pumping test data by Mills (1991) identified negative boundary effects and provides a first approximation for hydraulic conductivity of the aquifer pumped by the Goddard2 well. However, a non-leaky aquifer model does not closely match observed behavior. A conceptual model for the pumping test that is consistent with well and seismic data is a partially penetrating well in a sand stringer aquifer (in a floodplain environment) receiving leakage from fine-grained surrounding sediments and truncated by a fault (no-flow boundary). This conceptual model was used to simulate the Goddard2 pumping test with a discretization scheme in MODFLOW which accurately reproduces drawdown behavior at a pumping (or injection) well under non-radially

symmetric flow scenarios. Results are not unique but provide a framework for evaluating elements that are significant in local and regional ground-water flow, and provide a conceptual model to be tested and iteratively improved with new data and with future aquifer testing opportunities in the area.

INTRODUCTION

The lower Boise River valley relies almost entirely on ground water for public and domestic water supplies and for agricultural and industrial uses. Rapid population and economic growth have resulted in increasing demand for ground water while land-use changes from irrigated agriculture to urban uses are decreasing and redistributing the primary source of ground-water recharge which is infiltration from surface-water conveyance and application in the valley. Although the ground-water supply is not being depleted significantly in most areas at the present time, water-supply problems have occurred due to local contamination problems, to overdraughts in regions receiving little recharge, and to shallow wells going dry during drought cycles. Population growth is projected to continue for many years with continuation of fundamental changes in the hydrologic system.

Recent studies have advanced our understanding of the hydrogeologic framework of the valley (Squires et al., 1992; Wood, 1994) but these studies also point to the stratigraphic and structural complexities which affect ground-water flow and availability. Similarly, a model of ground-water flow in the western Snake River Plain was difficult to calibrate due to subsurface complexity and limited data on hydraulic parameters and interactions (Newton, 1991). Thus, two generic problems in the lower Boise River valley for quantitative analysis of ground-water resources locally and for modeling of ground-water flow regionally are: (1) characterizing the three-dimensional distribution of aquifer and aquitard units, significant geologic structures, and system boundaries; and (2) quantifying or estimating hydraulic parameters for and interactions between hydrologic units in hydrogeologic settings that include stratigraphic and structural complexities.

A location was selected in the northwest Boise area (Figure 1) to test methods for addressing these two generic problems where, during a pumping test of the Goddard2 water-supply well, negative boundary effects were recognized in the pumping well (Figure 2) but no drawdown was detected in the four observation wells monitored for the test (Mills, 1991). The hydrologic boundary effect may have been related to lateral changes in the producing zone and/or truncation of the aquifer by faulting. A deep seismic reflection profile in the vicinity (Figure 3) indicates faults are present in the sedimentary and subsedimentary volcanic units, but the seismic data do not image the stratigraphic level of the aquifer test (Wood and Anderson, 1981; Squires et al., 1992). Similarly, interpretations of the surface traces of faults in the vicinity of the Goddard well (Figure 1) are projections of subsurface data (Squires et al., 1992; Wood, unpublished data).

Although data from the Goddard2 well pumping test had been analyzed appropriately for engineering design purposes using standard simplifying assumptions, additional analysis was needed to quantify hydraulic parameters, interactions and dimensions based on complexities of the real system. Available subsurface information from wells in the vicinity of the Goddard2 well was not sufficient to define the subsurface sedimentary environment or to locate and describe geologic

structures which could be hydrologic boundaries. The approach to the Goddard2 problem, then, was divided into two parts that also address generic issues in the lower Boise River valley ground-water system: (1) use high-resolution seismic reflection profiling to develop an appropriate conceptual model for the hydrogeologic setting of the Goddard well area, and (2) develop a modeling method capable of analyzing a single-well test with boundary effects and complex hydrogeology.

HYDROGEOLOGIC SETTING

The study area for this report lies near the northern boundary of the western Snake River Plain which is a major, northwest-trending, late-Cenozoic rift basin that is filled, in the upper portion, primarily with lacustrine, deltaic and floodplain sediments of the Idaho Group (Malde and Powers, 1962; Malde, 1972; Kimmel, 1982). Where available, deep seismic reflection profiles and deep well data provide details of the shape of the subsediment volcanic "basement" (Figure 3 of this report; Wood and Anderson, 1981) and identify sedimentary environments within the basin fill (Figure 4 of this report; Wood, 1994). In the Boise area, Squires et al. (1992) interpreted subsurface sedimentary environments in the upper 1000 ft (300 m) of the system based on well data (Figure 5).

The northwest Boise study area (Figure 1) is underlain by a thin (generally about 50 ft [15 m] thick) veneer of coarse alluvium which overlies a 1500 ft to >2000 ft (450 m to >600 m) thick section of Idaho Group sediments. The water table commonly lies in the coarse alluvium, even where the valley topography is stepped up in terraces south of the Boise River. Producing zones in the Idaho Group generally are artesian, some of which flow, or used to flow, at the surface. Subsurface sedimentary environments in the Idaho Group in the vicinity of the Goddard1 and 2 wells have been interpreted by Squires et al. (1992; Figure 5, this report) to be deltaic/floodplain environments underlain by deep-water lacustrine environments (at the producing levels of the Goddard wells). Two significant northwest-trending normal faults which offset the volcanic "basement" in the only deep seismic reflection profile (Chevron IB-2 line) near the Goddard wells may cut Idaho Group sediments at producing zone levels or be continuous to nearly land surface in the vicinity of the Goddard wells (Figures 1 and 3, this report; Squires et al., 1992; Wood, unpublished data). However, the seismic data from the Chevron IB-2 line were not processed to image the upper 1000 ft (300 m) of the subsurface which is the region of interest for ground-water development.

HIGH-RESOLUTION SHALLOW SEISMIC REFLECTION PROFILE

High-resolution seismic reflection data were collected by the Boise State University Center for Geophysical Investigation of the Shallow Subsurface (CGISS) along three line segments (Figures 1 and 6) trending north-northeast from Chinden Boulevard to the Boise River at the Western Idaho Fairgrounds (WIFG) in the northwest Boise area (E 1/2 Section 25 T4N R1E). Total line length is about 4000 ft (1.2 km). The profile location was selected to cross the Eagle-West Boise fault or fault system at a high angle in order to locate it precisely and to recognize and measure displacement across the fault or faults. Also, working at the WIFG minimized urban interferences which allowed us to concentrate on optimizing data acquisition based on system characteristics; future lines run with urban interferences then can start from a set of known acquisition parameters and can better recognize and/or compensate for artificial effects. However, the CGISS line at the WIFG does not tie into any wells deeper than 300 ft (90 m) and stops about 1 mi (1.6 km) northeast of the Goddard1

and 2 wells.

SEISMIC DATA ACQUISITION

Seismic tests were conducted using two geometries: 'walk-away' noise spreads and multichannel common depth point (CDP) reflection profiles. Noise spreads are used primarily to test different source types and also to design acquisition parameters for the CDP profiles. CDP profiles are the principal final product used in structural and sedimentological interpretation of the area.

Near Surface Environment

Shallow seismic data acquisition is greatly affected by the surface and near surface environment (depths of 30 ft [9 m] or less). At the WIFG, surface materials ranged from hard-packed gravel parking lots and roads to clay-rich topsoil. Approximately half of the line was over grass fields underlain by both clay-rich topsoil and cobbly river deposits. The other half of the line was directly over packed gravel and/or river cobbles. A few asphalt roads also crossed the line. Where possible, geophones were planted in cracks in the asphalt, but generally, these areas did not contain receiver or shot locations. Source points near the river (north) end of the line were located on a loosely packed gravel road. Receivers at the north end of the line were planted directly in the very cobbly river bottom.

Noise Tests

Walk-away noise tests are conducted by laying out a short, closely spaced line of geophones and then walking away from the spread with source points spaced at intervals of the spread length away from the first receiver station. For the work presented here, a 3 ft (1 m) receiver spacing was used with a 48 channel system for a total receiver spread length of 330 ft (100 m). Walk-away noise tests were located at the WIFG such that subsurface coverage of the shot-receiver spreads was located near the center of the CDP line (Figure 6). Additional walk-away tests were conducted adjacent to the Goddard2 well.

A number of seismic sources were tested using the noise-spread geometry, including: sledge hammer, 12 gauge seismic Buffalo gun, 8 gauge electrically detonated black powder shells, a Bison EWG I, and Bison EWG III. The Bison EWG (elastic wave generator) sources are accelerated weight-drop sources. The EWGs were found to be superior to other sources because they provided good signal-to-noise ratios and also did not require drilling of shot holes.

In an effort to expand the areal coverage of the feasibility tests, walk-away noise tests also were conducted at one site adjacent to the Goddard2 well, located on the Whitney terrace (Othberg, 1994) about 1 mi (1.6 km) to the southwest of the WIFG. These tests were conducted adjacent to the nearby Settlers irrigation canal, and also in the bottom of the canal. Data collected adjacent to the canal displayed multiple reflections from the steep sides of the canal, rendering the data unusable. However, data collected from along the bottom of the empty canal did not contain these multiples. Reflections with strengths similar to those seen on the WIFG noise spreads appear on the Goddard noise spreads, indicating that data collection from within empty major irrigation canals may be a viable technique for use in future reflection experiments. Data from noise tests are given in

Dougherty et al. (1995).

Seismic Reflection Lines

Common depth point seismic reflection data were collected using three different sources along the CGISS line shown in Figures 1 and 6. Initially, a short test line was run in one of the grass fields at the WIFG using a sledge hammer source. A long line was then run using the Bison EWG III from Chinden Avenue to midway across the Boise River. Receiver spacing of 16.5 ft (5 m) was used for the EWG III line and a total of 122 shots were recorded. Shot spacing varied from 16.5 to 33 ft (5 to 10 m) along the EWG III line. A somewhat shorter line was run with 10 ft (3 m) receiver spacing and the EWG I for a source (northern segment of seismic line in Figure 6). Shot spacing for the EWG I line was 10 ft (3 m) and total of 235 shots were collected for that line.

CDP seismic reflection data were processed using standard industry processing techniques contained within PROMAX, a commercially available seismic processing software package. The EWG III line presents the best image of stratigraphy and structure at depths of approximately 150 to 2300 ft (45 to 700 m) (Figure 7a); only some of the features seen in the EWG III profile could be identified in the EWG I data even though they were collected along the same line. For this site, near-surface coupling of the lighter weight-drop source (60 lbs [27.3 kg] for the EWG I hammer vs. 550 lbs [250 kg] for the EWG III hammer) did not seem to be sufficient for an adequate seismic section. Data quality from the EWG lines is moderate, but the EWG III line provides sufficient subsurface image detail and clarity to interpret four depositional zones or environments. An interpreted EWG III section is shown in Figure 7b.

RESULTS

At the WIFG, the depth range for imaging with high-resolution shallow seismic reflection is between about 150 and 2300 ft (45 and 700 m) BLS (Figure 7). This range includes most of the region between the shallow, unconfined alluvial aquifer and the subsediment acoustic basement (reflector at the top of the volcanic section). Also, image clarity decreases toward the northern end of the profile presented here where source coupling was poor. The seismic reflection profile generated in this study images features that correlate well with the Chevron IB-2 line where the two are in close proximity (Figures 1, 3 and 7).

Stratigraphic Interpretation

Four seismic stratigraphic units (e.g., Mitchum et al., 1977; Brown and Fisher, 1977) are identified in the high-resolution seismic reflection profile from this study (Figure 7b). Lithologic or sedimentary environment interpretations are based on correlations with previously identified units and on image patterns correlated with well data in this and other basins. The orientation of the seismic profile is at a high angle to the orientation of the basin axis and direction of sediment influx. While optimal for structural interpretation, this orientation is not the most favorable for interpretation of sedimentary environments from seismic reflection profiles.

The four seismic stratigraphic units interpreted from the seismic profile developed in this study are, from older to younger: unit 1, acoustic basement reflector correlated with the top of the middle

Miocene volcanics that underlie the Idaho Group sedimentary section (Wood and Anderson, 1981; Wood, 1994); unit 2, sedimentary unit with discontinuous reflectors interpreted to be a deep-water and prodelta lacustrine environment; unit 3, sedimentary unit interpreted to be a delta-plain sand; and unit 4, sedimentary unit interpreted to be a floodplain/delta? environment. Additional descriptions are given below.

Unit 1: Acoustic Basement

A strong reflector can be traced across much of the profile from about 1400 ft (460 m) depth in the north to about 2000 ft (600 m) depth in the south (Figure 7). Based on character and position, this reflector is correlated with the top of middle Miocene volcanics that underlie the Idaho Group elsewhere within and at the margins of the western Snake River Plain including locations confirmed with well data (Wood, 1994). This interpretation is consistent with that of Squires et al. (1992) for the Chevron IB-2 line approximately 1 mi (1.6 km) west of the CGISS line (Figure 1). Overall the volcanics are offset down-to-basin by normal faults (see below) and have apparent basinward dips of about 11° north of the Eagle-West Boise fault (Figure 7b).

Unit 2: Prodelta/Deep-Water Environments

Unit 2 overlies the volcanic basement and ranges in thickness between about 660 ft (200 m) to the north and 1100 ft (330 m) to the south in the CGISS line (Figure 7). Discontinuous reflectors within unit 2 generally have southerly apparent dips that likely have been influenced by the basinward down-stepping structures. Lateral extent of these reflectors range from 1500 ft ($\geq$450 m) to 2500 ft ($\geq$750 m), although it is possible that the widths of reflectors are artificially limited by surface effects influencing data quality.

Reflectors in unit 2 are interpreted to be generated by sand bodies that are surrounded by dominantly fine-grained sediments in deep-water and/or prodelta sedimentary environments. It is difficult to distinguish between these environments given the orientation of the seismic line. However, units with similar seismic expression have been correlated with deep-water and/or prodelta sedimentary environments in the western Snake River Plain (Wood and Anderson, 1981; Squires et al., 1992; Wood, 1994) and in other basins (e.g., Changsong et al., 1991; Brown and Fisher, 1977). Also, these environmental interpretations for unit 2 are consistent with a position between subsiding basement and the interpreted overlying deltaic environment (unit 3).

Basining during the deposition of unit 2 occurred progressively or perhaps in two stages as indicated by greater southward apparent dips in the lower part of the unit (Figure 7b). This relationship is best imaged in the region between CDP ranges 200 m to 300 m (CDP range is lateral distance from south end of seismic line - see Figure 7), and depths 250-450 m (825-1500 ft). In particular, the apparent dip of a reflector at CDP range 275 m and depth 375 m is about 11° while the apparent dip of a reflector above, at CDP range 275 m and depth 300 m, is about 3°. These findings within the basin are similar to those of Kimmel (1982) who noted that increasing dips on older sediments at the margins of the basin indicated subsidence during deposition.

Unit 3: Delta-Plain Sand

Unit 3 is characterized by a strong reflector at about 725 ft (220 m) depth at the southern end of the profile rising to at least 660 ft (200 m) depth before being lost toward the north end of the line. Lack of continuity may be due to erosional removal by the overlying unit, to data acquisition problems (i.e., signal clarity decreases in the profile to the north), or to lack of original presence at the north end of the line. Thickness of unit 3 may be approximately 50 ft (15 m) based on the elevation difference between the tops of the unit 3 reflector and the first weaker reflector of unit 2 below. The interpretation of unit 3 being a delta-plain sand environment is based on the strength of the reflector (S.H. Wood, personal communication, 1995), its position between subaerial and submerged environments, and the slight erosional truncation of the underlying unit - see contact in Figure 7b at depth 230 m (760 ft) and CDP range 150 m where unit 3 has an apparent basinward dip of about 2° and the underlying reflector in unit 2 has an apparent basinward dip of about 7°.

Unit 4: Floodplain/Delta?

Unit 4 is the uppermost unit in the profile and it has distinctive dipping reflectors of limited lateral extent that overlie, or are adjacent to, reflectors with differing apparent dip directions. Apparent dips on the dipping reflectors commonly range between 2° and 15°, although an apparent dip of about 33° occurs at about CDP range 525 m and depth 100 m. The uppermost 150 ft (45 m) of signal is not recovered and so it is not certain if this unit continues upward to the base of the shallow, unconfined alluvial aquifer which is generally about 50 ft (15 m) thick in this vicinity based on drillers' logs. The occurrence of the variably oriented dipping reflectors decreases downward to the strong reflector (unit 3) below, so it is possible that there is a transition to a different (upper delta plain?) environment immediately above unit 3. Thickness of unit 4 is at least 330 ft (100 m).

The paleoenvironment of unit 4 is interpreted to be a floodplain with a meandering stream depositing cross-bedded sands in variable orientations. Such sand bodies occur within laterally restricted belts strongly associated with thick fine-grained sediments generated in overbank, vertical accretion deposits. Figure 8 is a highly simplified schematic diagram showing general distribution of sand and fine-grained sediments for a meandering stream in a floodplain environment (Walker and Cant, 1979; Coleman and Prior, 1982). Figures 9-10 show drillers' lithologic logs from wells >500 ft (>150 m) deep in the vicinity of the Goddard wells with characteristics broadly consistent with meandering streams (e.g., Cant, 1982): thick sand and fine-grained units, and limited continuity between sand units across depositional strike (Figure 10). The association of thick sand and thick fine-grained units of limited lateral extent also is consistent with observations by Malde (1972) and Smith et al. (1982) on floodplain lithologic associations in the Glenns Ferry formation at exposures in the western Snake River Plain.

Structural Interpretation

The orientation of the seismic profile was intended to cross the strike of the projected Eagle-West Boise fault or fault zone at a high angle (Figure 1) because a major objective of this study was to identify the location and subsurface character of faults that might be negative hydrologic boundaries. Unfortunately wells deeper than 300 ft (90 m) are not located near the CGISS seismic line so independent lithologic control is not available. However, faults have been interpreted in the CGISS

seismic profile (Figure 7), with varying degree of certainty, based on abrupt offset of reflectors (e.g., CDP range 600 m, depth 500 m [1500 ft]), drag at offsets (e.g., at CDP range 580 m, depth 400 m [1300 ft]), and vertical consistency of offset indicators and sense of offset within the profile. With few exceptions (e.g., antithetic fault at CDP range 375 m, depth 600 m [2000 ft]), faults are normal faults with the downthrown block on the south (basinward) side.

Apparent offsets range from barely recognizable to approximately 165 ft (50 m) on the Eagle-West Boise fault which cuts the basement reflector at about CDP range 450 m in Figure 7b and is identified by Squires et al. (1992) in the Chevron IB-2 line. Several faults can be traced up section to the unit 3 reflector with reasonable certainty based on apparent offsets and abrupt changes in dip, although offsets on these faults generally decrease upsection to folds or barely recognizable breaks (Figure 7b).

The pattern of decreasing offset upward across a fault is consistent with progressive fault activity (basining) during deposition. In this regard, one fault terminates upward toward a fold (range 350 m, depth 420 m [1400 ft]) which appears to be the lower expression of a hinge between two structural blocks: a block to the north of this hinge which appears to be a graben wedge with reflectors dipping toward the center of the wedge (between the hinge and the Eagle-West Boise fault), and a block to the south of the hinge where the reflectors are subhorizontal or dipping southward from it. Another hinge between blocks (where dips steepen to the south) occurs in the vicinity of the fault at range 200 ± 25 m.

CONCEPTUAL MODEL

General hydrogeologic implications of the seismic and limited well data in northwest Boise in the vicinity of the Goddard wells are: (1) most wells below the shallow, unconfined alluvial aquifer are completed in seismic stratigraphic unit 4 where thick sands are not continuous but are relatively abundant; (2) sand-body dimensions likely are at least several miles long (in the general basin-axis direction of NW-SE), are linear, and are thin (50-100 ft [15-30 m] thick) compared to the thickness of the section as a whole; (3) sediments generally are unlithified and relatively uncompacted (based on descriptions in drillers' logs), so porosity and permeability of fine-grained sediments will tend toward higher values rather than lower values within expected ranges and can contribute leakage to otherwise isolated permeable sand stringers; (4) the unit 3 sand may be a relatively continuous sheet; (5) sands seen as reflectors surrounded by fine-grained sediments in the prodelta/deep-water environment of unit 2 may be segments of channels that funneled turbidity currents to the basin floor but that had a high potential for preservation of relatively thick sands, and which likely have somewhat similar overall geometry to the sand bodies of unit 4 (e.g., Walker, 1979; Berg, 1982); and (6) faulting in the upper part of the sedimentary section may disrupt ground-water flow where productive units are affected, but such disruption likely only occurs across major faults.

Within the context of the seismic stratigraphy of the CGISS profile at the WIFG, the producing zone of the Goddard2 well occurs in seismic stratigraphic unit 4. The base of unit 4 at the south end of the CGISS profile is about 1960 ft above mean sea level (>660 ft or >200 m depth, Figure 7b) which is lower than the base of the Goddard2 well producing zone (>2100 ft elevation, see Figure 11).

Also, the southward down-to-basin sense of displacement likely would lower the base of unit 4 further to the south of the CGISS line. Unit 4 is interpreted here to be a floodplain/delta? sedimentary environment and the Goddard2 well is interpreted to be completed in it. Squires et al. (1992) interpreted a deep-water environment for sediments below about 2200 ft elevation (Figure 5b) in the Goddard wells and nearby wells based on analysis of drill cuttings and geophysical logs in addition to drillers' lithologic logs. Although the general lithologic characteristics of thick sands and clays may be similar for sands preserved in deep-water (prodelta channels feeding turbidites) and meandering stream deposits in a floodplain, the additional information from seismic data on stratigraphy and structural relationships indicate the deep-water environment is below the producing zone at the Goddard2 well.

The dimensions of the sand unit tapped by the Goddard2 well, based on drillers' logs (Figures 9-11) and high-resolution seismic reflection data (Figure 7), likely are limited in width (<5000 ft [1500 m] and perhaps <2000 ft [<600 m]) and thickness ($\leq$100 ft, $\leq$30 m). Length continuity of several miles or more may be inferred by possibly correlative thick sands in wells along the NW-SE trend of sediment influx (Figure 9).

The lateral limits of the producing sand at the Goddard2 well (Figure 10) may be explained by the geometry of primary sedimentological features (meandering stream channel, Figure 8) rather than structural offsets, although structural offsets may truncate the sand or influence the ground-water flow system at a boundary nearby. That is, based on the scarcity of significant structural displacements in unit 3 (and by inference, unit 4) in the CGISS seismic reflection profile nearby to the northeast (Figure 7b), faulting likely is not the sole or the primary cause for the lack of lateral (NE-SW) continuity of sand units in the region surrounding the Goddard wells.

The length of the producing sand is not easily defined or limited by existing well or seismic data. Thick sands in wells up depositional trend to the southeast of the Goddard wells may correlate with the sand unit screened in the Goddard2 well. In particular, potentially correlative sand units in the Capitol Securities wells 3 and 5 (Figure 9) are approximately 70 to 100 ft (21 to 30 m) higher than in the Goddard wells at upstream distances of approximately 1.3 to 2 mi (2080 to 3200 m). These distances convert to stream gradients of approximately .006-.007 assuming a sinuosity index of 1.6-1.7 which is in the >1.5 range appropriate for a meandering stream (Morisawa, 1985). A gradient of .006-.007 is near the upper limit for meandering streams (Morisawa, 1985). The lack of a potentially correlative sand in the Fisk well (Figure 9) is neutral evidence for the continuation of a sand stringer to the southeast of the Capitol Securities 5 well.

To the northwest of the Goddard wells (Figure 9), the Garden City 8 well is about .6 mi (1050 m) in the downstream direction and has a thick sand sequence approximately 100 ft (30 m) below the sand unit screened in the Goddard2 well. Using assumptions similar to those above, a gradient of .02 results which is too high for a meandering stream (Morisawa, 1985). However, the Garden City 8 well also is northeast of the surface projection of an unnamed normal fault (Wood, unpublished data: fault B in Figures 1 and 3) which would place this well in the footwall (relatively higher) block relative to the Goddard wells. Any gradient calculations between the Goddard and Garden City 8

wells then would be minimum values if vertical offset occurred across the fault at the stratigraphic level of the Goddard2 well production zone. So, two lines of reasoning (gradient and faulting) suggest that sands at the bottom of the Garden City 8 well are not correlative with the screened interval in the Goddard2 well. Also, correlation of the Goddard2 screened interval with sands in 2058-1978 ft interval in the Settlers well (Figure 9) is not likely due to a stream gradient estimate exceeding .01.

We interpret that the producing sand zone in the Goddard2 well is surrounded by clay, silty clay, and silty sand that, as an aggregate, are not impermeable and will yield water from storage because drillers' logs indicate fine-grained sediments are not lithified or highly compacted, and because analytical modeling of the system as non-leaky does not closely resemble drawdown behavior if reasonable storativity values are used (discussed below). Other sand bodies with geometry similar to that of the aquifer tapped by the Goddard2 well (length > width > thickness) are interpreted to be distributed as separate units surrounded by finer grained sediments within the floodplain environment of the lower Boise River valley aquifer system, although some overlap and hydraulic continuity between sand stringers is possible (Cant, 1982; Fogg, 1989). Figure 8 is a highly simplified schematic representation of this type of environment.

ANALYSIS OF PUMPING TESTS

Well construction (Figure 11) and pumping tests are described below. Two types of aquifer tests were conducted with the Goddard2 well in 1991 (Mills, 1991): a step-drawdown test and a constant-rate pumping test during which the average pumping rate was 1714 gpm (108 L/s). The engineering analysis of Mills (1991) is extended here by modeling test behavior in the context of a conceptual model (developed above) that is consistent with the hydrogeologic environment, and with well responses and lack of response during the constant-rate test. The following well construction and test facts are useful for test analysis. Total depth of the Goddard2 well is 551 ft (167 m) with a 30-slot, 10 in (.25 m) diameter screen in the upper 75 ft (23 m) set from 475 to 550 (144 to 167 m) BLS in a 100 ft (30 m) thick sand. Casing diameter above the screen is 18 in (.45 m). For both aquifer tests, a line-shaft turbine pump was set at 200 ft (60 m) BLS which is about 275 ft (about 83 m) above the screen. Flow rates were measured through an orifice weir with a lower calibration threshold of 600 gpm (38 L/s) (Mills, 1991).

WELL LOSSES

Well construction is consistent with minimal well losses during pumping of the Goddard2 well. This is important to establish if hydraulic behavior of the aquifer will be interpreted from drawdown responses at the pumping well alone. Two lines of evidence are developed below which indicate that well losses do not significantly influence drawdown behavior at the Goddard2 well: (1) engineering calculations on construction dimensions predict laminar flow into and up the well; and (2) step-test performance demonstrates that non-linear well losses are not detectable.

Analysis of well construction (Figure 10) and inflow conditions at the well screen support the interpretation of laminar flow in the vicinity of the well screen. For a cylinder of 75 ft (23 m) length and 10 in (.25 m) diameter, the surface area is 196.4 ft^2 (18 m^2). For a 30 slot screen, 41% of the

surface area is open for flow (Driscoll, 1986). Entrance velocity to the well then is

$$v_e = Q/A$$

where v_e is entrance velocity to the well screen
Q is well pumping rate
A is cross-sectional area, and

where, for the most extreme case tested, Q is 1714 gpm or 229 ft^3/min (108 L/s) and A is .41 x 196.4 ft^2 or 80.5 ft^2 (7.4 m^2). So,

$$v_e = Q/A = (229\ ft^3/min) / (80.5\ ft^2) = 2.8\ ft/min = .047\ ft/s\ (.014\ m/s)$$

which is below the design limit (i.e., within the laminar flow range) for relatively permeable aquifers (US EPA, 1975, p. 90; Driscoll, 1986, p. 996).

Similarly, flow up the well from the screen to the pump intake was laminar and incurred minimal pipe loss. Flow velocity up the casing equals Q/A, where Q is 1714 gpm or 229 ft^3/min (108 L/s) and A is the pipe cross-sectional area (1.77 ft^2 [.16 m^2] for casing diameter of 18 in [.45 m] above the screen). Flow velocity, then, is about 129.6 ft/min or 2.16 ft/s (.65 m/s). Head loss in the Goddard2 well is expected to be less than .3 ft or .09 m (i.e., <.1 ft/100 ft of pipe) during a constant-rate test at 1714 gpm (108 L/s) based on the nomogram provided by Driscoll (1986, Appendix 13K) to determine head loss knowing pipe diameter or flow rate and flow velocity.

STEP TEST

A five-step test (Mills, 1991) was conducted with discharges of 350? gpm (22? L/s), 600 gpm (38 L/s), 1000 gpm (63 L/s), 1300 gpm (82 L/s), and 1500 gpm (95 L/s) for time periods ranging from 15 min to 73 min and, with the last four steps lasting more than 50 min each (Table 1). Pumping was continuous across steps, and the total pumping period for the test was 255.5 min. Initial water level was about 40 ft (12 m) below top of casing, 160 ft (48 m) above the pump and 430 ft (130 m) above the screen. Total drawdown at the end of the test was approximately 100 ft (30 m) (Table 1). In addition, data from the constant-rate pumping test at 1714 gpm (108 L/s) (Table 2) are used to extend the step-test analysis to the pumping rate of the constant-rate test (Table 1, Figure 12b).

Specific capacity values from the step test ranged between 14.9 and 16 gpm/ft (3.1 and 3.3 L/s-m) of drawdown for the last four steps with time intervals between 50 and 73 min (Mills, 1991). Results are essentially the same if specific capacities are normalized for a uniform time of pumping per step and if pre-existing pumping trends are projected into subsequent pumping steps (Table 1; Figure 12b). Specific capacity did not decrease with increasing pumping rate as would be expected if non-linear well losses were associated with pumping at this well (e.g., Hantush, 1964). Rather, specific capacity remained essentially constant with increasing pumping rate. These data indicate that: (1) turbulent or non-linear well losses are not recognizable in the drawdown behavior of the Goddard2 well in the range of pumping rates examined by the step test and for the constant-rate test at 1714

gpm (108 L/s) ("step" 6 of Table 1; Figure 12b); and (2) the specific capacity of the Goddard2 well is about 15 gpm/ft (3.1 L/s-m) of drawdown at 50 min of pumping (Table 1).

CONSTANT-RATE TEST

The Goddard2 well was pumped for 8 hr at an average rate of 1714 gpm (108 L/s) on February 28, 1991. During the test (Mills, 1991), flow rate drifted downward a number of times and pump rpms had to be adjusted upward to return the pumping rate to its long-term average rate (Table 2). Four observation wells were monitored for drawdown effects; one well (Goddard1) was 40 ft (12 m) from the pumping well, the other three wells are located approximately 5000 ft (1500 m) from the pumping well (Figures 1 and 11). Lithologic logs and screened intervals for the observation wells are given in relation to the pumping well in Figure 11. Data and analysis presented by Mills (1991) indicate that none of the four observation wells responded to pumping at the Goddard2 well. This is not surprising because the screened intervals in three of the observation wells are at significantly different elevations than the screened interval in the Goddard2 well and, again, three of the wells are 5000 ft (1500 m) from the Goddard2 well (Figure 11), and the length of the test was only 8 hr.

Engineering Estimate of Transmissivity

Semilog straight-line analysis (Cooper and Jacob, 1946) of the preboundary drawdown data for the Goddard2 well gave a transmissivity value of 39,000 gpd/ft (3.6 ft^2/min, .0055 m^2/s), and apparent transmissivity of 22,000 gpd/ft (2 ft^2/min, .003 m^2/s) was given for late-time boundary-affected drawdown behavior (Mills, 1991). Negative boundary effects at the Goddard2 well appear to be pronounced after about 180 min (Figure 2). Changes in aquifer geometry, aquifer properties or faulting were suggested as possible causes for the boundary effects (Mills, 1991). Recognizing that the purpose of the pumping test analysis was to estimate well productivity and determine long-term pumping rates and levels, the preboundary estimate of transmissivity using semilog straight-line analysis is useful as a first approximation. If the aquifer thickness is taken to be 100 ft (30 m) by including sand below a thin clay seen in the nearby Goddard1 well (Figure 11), then an initial estimate for hydraulic conductivity of the aquifer is .036 ft/min (.00018 m/s).

Evaluation of Non-Leaky Aquifer Model

One assumption of semilog straight-line analysis is that the aquifer does not receive leakage (Cooper and Jacob, 1946). Subsurface geological and geophysical data indicate that this assumption may not be valid for the Goddard2 well environment. One approach to testing the non-leaky aquifer assumption underlying the Cooper-Jacob straight-line method is to see if log-log plots of Theis curves (with T=3.6 ft^2/min [.0055 m^2/s] from the straight-line analysis and with reasonable values of storativity) compare favorably with the observed data at the Goddard2 well (Figure 13). The Theis curve best fitting the observed data prior to boundary effects is generated with an unrealistically low specific storage value of $S_s = 10^{-8}$ ft^{-1} ($3.3x10^{-8}$ m^{-1}), or a storativity value of $S=10^{-6}$ for a 100 ft (30 m) thick aquifer. Other Theis curves are not close fits to the data. One or more of the Theis model assumptions need to be reevaluated.

In addition, it is difficult to take the analysis of the Goddard2 drawdown data further because the post-boundary data never satisfy the u criterion ($u < .01$) where $u = r^2S/4Tt$. That is, late-time

analysis with the semilog straight-line method (Cooper and Jacob, 1946) is not justified because non-linear terms in the well function cannot be ignored. For reasonable values of storativity and reasonable distances to a no-flow boundary, the time, t_c, at which the u criterion would be satisfied can be estimated (Table 3) by considering the components of u when u = .01:

$$u = .01 = \frac{r_i^2 S}{4Tt_c} \quad ; \quad t_c = \frac{r_i^2 S}{4T(.01)} = \frac{r_i^2 S \ ft^2}{.144 \ ft^2/min}$$

where r_i is the distance to an image well that is twice the distance from the pumping well to the boundary, S is storativity, and T = 3.6 ft^2/min (.0055 m^2/s) as a first approximation from the pre-boundary straight-line analysis.

It can be seen from Table 3 that t_c values exceed the length of the pumping test for most possible combinations of storativity and distances to a boundary. And for a boundary at 50 ft (15 m) or 250 ft (75 m), numerical modeling results of drawdown at a pumping well having the Goddard2 characteristics and pumping at 1714 gpm (108 L/s) from a non-leaky aquifer with T = 3.6 ft^2/min (.0055 m^2/s) were not similar to the actual test results, and boundary effects were evident sooner (i.e., <180 min) than they appeared during the actual test (Figure 2).

Although there are problems with the inherent assumption of a non-leaky aquifer and with application of the semilog straight-line method for interpretation of aquifer parameters and late-time boundary analysis, we may use the interpreted transmissivity value from the pre-boundary data as a first approximation. And we can use the conceptual model of the hydrogeologic setting of the Goddard wells as the basis for a numerical model that may better explain the observed hydraulic behavior during the constant-rate pumping test at the Goddard2 well.

NUMERICAL MODEL

A numerical modeling approach is used here to simulate behavior at the Goddard2 well during the constant-rate test while incorporating major features of the hydrogeologic system consistent with the conceptual model developed above. Before proceeding with the model configuration and results, however, it is important to note that the model is not presented here as a unique solution but rather as one realization that is consistent with features that are recognized to be part of the lower Boise River valley aquifer system and part of this particular test (e.g., fault or negative boundary, leakage, finite aquifer with geometry related to paleoenvironment). That is, our purpose is to demonstrate a method that can incorporate some of the complexity known to exist in the real system, and thereby offer a starting point in an iterative process to help guide data gathering to refine our understanding of parameters, interactions and dimensions that are important for simulating the behavior of the aquifer system in the lower Boise River valley. The opportunity for follow-up verification and model improvement should be taken if new wells are placed in this area.

Modeling Non-Symmetric Flow to a Well with MODFLOW

MODFLOW (McDonald and Harbaugh, 1988) is the numerical modeling code used to simulate drawdown behavior at the Goddard2 well during the constant-rate test. MODFLOW is a finite-

difference code that uses a rectilinear grid system. Appendix A demonstrates a discretization scheme in MODFLOW which accurately simulates drawdown at a pumping well under non-radially symmetric flow conditions, as well as in layered, leaky systems with a partially penetrating well (Barrash and Dougherty, 1995). In this scheme (Figure 14): (1) the well cell is square, in plan view, with x- and y-length dimensions equal to the well diameter; (2) cells adjacent to the well cell have very small widths (typically 0.2% to 3% of the width of the well cell); and (3) cells outward from the cells adjacent to the well cell have increasing cell widths with an expansion factor, α (Reilly and Harbaugh, 1993), of ≤ 1.5 where α is the ratio of lateral distance between neighboring nodes, starting with the cell adjacent to the well cell. This approach captures steep and rapidly changing gradients near the well and closely approximates curvature of head or drawdown contours despite the rectilinear grid geometry. Vertical discretization and time discretization are treated as in other modeling problems to achieve accuracy and convergence.

Model Configuration

Based on the conceptual model presented above, the aquifer tapped by the Goddard2 well is modeled as a 100 ft (30 m) thick, 30,000 ft (9.1 km) long sand body whose width is truncated by a fault on the northeast side such that the modeled aquifer width is 1280 ft (390 m). The aquifer is surrounded by fine-grained material that is 700 ft (212 m) thick overall and 300 ft (90 m) thick above and below the sand stringer aquifer (Figure 15). The Goddard2 well is placed 13,000 ft (3.9 km) from the northwest end and 17,000 ft (5.1 km) from the southeast end of the sand stringer aquifer. Hydraulic parameters are constant within these two hydrologic units and are given in Figure 16. The aquifer is modeled as having isotropic hydraulic conductivity (.031 ft/min, .00016 m/s); the aquitard is given a 5:1 vertical to horizontal anisotropy ratio (.0003 ft/min:.00006 ft/min [1.5×10^{-6} m/s:3×10^{-7} m/s]). Outer boundaries of the model domain are no-flow boundaries.

The long axis of the aquifer is aligned parallel to the long axis of the western Snake River Plain and parallel to a fault (no-flow boundary) that is oriented vertically, that fully cuts the flow domain laterally and vertically, and that is located 500 ft (151 m) northeast of the Goddard2 well (Figure 15). This fault may be the significant fault recognized by Wood (unpublished data; Figures 1 and 3, this report). Such a fault associated with a river course may be a reasonable coincidence because channels can be guided by active faults (e.g., Scott et al., 1991) and we know from the CGISS line that some faults were active through most or all of the period from unit 1 through at least unit 3.

The model domain was discretized into 30 layers of 80 x 99 cells per layer. Thicknesses of different layers vary with finer discretization at material property boundaries and at the bottom of the partially penetrating pumping well (Figure 16). Tables 4 and 5 list the dimensions of the grid and layers, respectively. The Goddard2 well partially penetrates the 100 ft (30 m) thick aquifer to a depth of 75 ft (23 m) within the aquifer, and the well diameter is 10 in (.25 m), as given in well completion records. The aquifer is comprised of 12 layers and the aquitards are comprised of 9 layers each where they are above and below the aquifer. The well is located at row-column position [31,50] in layers 10 through 17 (Figure 16). Pumping is apportioned by percent thickness of a given layer relative to total open interval (75 ft, 23 m) in the aquifer.

Both time and space (near the Goddard2 well) are discretized very finely in this model to achieve convergence under severe early time conditions where more than 90 ft (27 m) of drawdown occur within the first 2 min of the pumping test (Table 2). The SIP solver is used with 1000 iterations available per timestep, and with the fairly strict convergence criterion of .0001 ft (.00003 m). Cells adjacent to the well cell have widths of .0016667 ft (.0005 m), or 0.2% of well-cell width. Even though the pumping rate is kept constant at the long-term average of 1714 gpm (108 L/s) during the simulation, the test is simulated over four time periods lasting a total of 561 min with 115 time steps, in order to keep the duration of each time step short enough to allow convergence (Table 6). The first period is 1min long and is divided into 30 time steps.

Drawdown in the well was figured by using a weighted average of drawdowns in the 8 layers which had well segments (Figure 16, Table 5). The weighting factor for each layer was the thickness fraction of open interval for a given layer having a well segment:

$$\Delta s = \sum \Delta s_i \; ; \quad \text{where } \Delta s_i = \Delta s * (b_i/75 \text{ ft})$$

where s is drawdown measured in the well, s_i is drawdown simulated in a given layer, and b_i is the thickness of a given model layer containing a well segment.

During the actual test it was noted that the pumping rate was adjusted upward a number of times to counter downward drift (Figure 17, Table 2). In general, higher curve segments were used to guide matches in preference to lower segments that ended with abrupt jumps at times of flow-rate adjustment (Figure 17). However, the first few data points likely represent anomalously high drawdown due to a higher-than-average pumping rate while the discharge system was being filled and until a steady back pressure was established (e.g., Barrash and Ralston, 1991; Squires et al., 1993). Modeling efforts did not attempt to duplicate test data exactly but tried to match basic data trends.

General constraints on the geometry of hydrogeologic units were provided by drillers' logs, seismic sections, and literature (see Conceptual Model above). Hydraulic parameters were selected from within expected ranges (Freeze and Cherry, 1979) after hydraulic conductivity for the aquifer was initially set at .036 ft/min (.00018 m/s) (Mills, 1991). This value subsequently was decreased to .031 ft/min (.00016 m/s) as leakage, specific storage values and geometrical factors were added to the model. The aquitard will supply water from storage and was given impermeable boundaries 300 ft (90 m) above and below the aquifer, and $\geq$79,000 ft (23.9 km) laterally beyond the aquifer. A uniform head distribution was used for initial conditions.

In addition to matching behavior at the Goddard2 well (Figure 17), the model is consistent with the lack of response at the Millstream and Westmoreland wells that are located northeast of the fault (Figure 1). Also, evaluation of drawdown in the model for the Settlers well, outside the aquifer about 1500 ft (.45 km) southwest and 5000 ft (1.5 km) northwest of the Goddard2 well, indicates no drawdown is expected there. Evaluation of drawdown for the Goddard1 well similarly indicates minimal drawdown could be expected by the end of the test. Evaluation of drawdown at the

locations of the Capitol Securities wells 5 and 6 (Figure 9) in the aquifer indicates that no drawdown would be expected (CS5 was not monitored and CS6 was not yet emplaced at the time of the Goddard2 test). Similarly, pumping from CS5 would not have affected the Goddard2 well during the test.

Sensitivity Analysis

Limited sensitivity analysis was performed as part of this study. In the trial-and-error process of matching observed pumping test behavior with simulated behavior, (predictable) findings were: magnitude of drawdown is very sensitive to aquifer permeability; curve shape is sensitive to aquifer storativity and leakage from surrounding aquitard material; and late-time negative boundary effects are sensitive to the location of the impermeable fault boundary. Sensitivity to length of the sand stringer aquifer was checked by running simulations with the northwest and southeast ends of the aquifer respectively at 3,000 ft (.9 km) and 17,000 ft (5.1 km) from the pumping well, and at 22,000 ft (6.7 km) and 21,000 ft (6.4 km) from the pumping well. These different lengths for the aquifer had very little influence on the simulated drawdown curve when the same input parameters (Figure 16) were used.

We recognize that additional analysis could be performed on aquifer dimensions and attitude, on aquitard parameters and magnitude of anisotropy, on variability of parameters and dimensions for the aquifer and aquitard, and on initial conditions and boundary conditions. However, because of the relatively large number of dimensions and parameters that are not directly constrained by subsurface data or pumping test reponses, evaluation of sensitivity through many permutations and combinations of dimensions and parameters would be unwarranted at this time. Indeed, the modeling objective of this study was method testing rather than exhaustive modeling analysis.

SUMMARY

The main thrusts of this study were to: (1) evaluate high-resolution seismic reflection as a tool for imaging stratigraphic and structural detail at depths relevant to hydrogeologic system interpretation and modeling, and (2) develop a method for analyzing aquifer-test behavior at a pumping well which can incorporate hydrogeologic complexities that cannot be included in analytical or radially symmetric numerical models.

Results presented here demonstrate that high-resolution seismic reflection data are effective at imaging hydrologically important strata, the geologic environments in which they occur, and geologic structure. Surface sources such as the EWGs (elastic wave generators) used here provide sufficient energy for imaging shallow, hydrologically important strata. However, as with all shallow subsurface seismic sources, degradation in data quality near the present day Boise River indicates that EWG source coupling is highly sensitive to near surface conditions. At locations more distant from the present-day Boise River channel, source coupling would most likely improve, leading to even higher quality seismic reflection data.

Our results indicate that high-resolution seismic reflection is effective for imaging reflectors and patterns of reflectors that may be interpreted as stratigraphic units and, perhaps more tentatively, as

sedimentary environments. Structural style is clearly imaged, and apparent dips and offsets can be measured. Acoustic basement, structures offsetting acoustic basement, and character of deep-water facies are similar in the CGISS profile at the WIFG and the Chevron IB-2 line about 1 mi (1.6 km) to the north.

The NE-SW seismic line orientation used here was favorable for imaging structure but was less favorable for imaging sedimentary environment features because the strikes of faults are subparallel to the direction of basin-filling sediment transport. Depth range of imaging capability with the seismic data acquisition configuration used in this study is between about 150 ft (45 m) and about 2300 ft (700 m) BLS. Acquisition and processing parameters determined in this study should be generally applicable to future high-resolution seismic work in the valley.

Images from the CGISS high-resolution seismic reflection profile at the WIFG are consistent with a stratigraphic sequence of, from older to younger: volcanics, prodelta/deep-water lacustrine deposits, delta-plain sand, and floodplain/delta? sediments. Based on seismic data and available nearby deep well data, the Goddard2 well likely is screened in a relatively long, narrow sand body of the floodplain environment. Also a normal fault is projected to offset this aquifer based on a significant fault seen in the Chevron IB-2 line (south of the CGISS line). Significant elements of this conceptual model were generalized in a numerical model where a vertical fault (no-flow boundary) truncates a 30,000 ft (9 km) long aquifer (with simple, tabular geometry and uniform hydraulic parameters) that receives leakage from surrounding aquitard material (with uniform hydraulic parameters, including vertical-to-horizontal anisotropy of permeability).

Results from an 8 hr constant-rate pumping test at the Goddard2 well, where only the pumping well had measurable responses during the test, were matched with simulations generated by a numerical model based on the conceptual model of the hydrogeologic system in the vicinity of the Goddard wells. A discretization scheme in MODFLOW developed for this type of application can accurately reproduce steep, rapidly changing gradients at a well, such as the >90 ft (>27 m) of drawdown that occurred in the Goddard2 well in less than 2 min. Modeling of the hydrogeologic system in the region of the Goddard wells may be refined with future seismic work, drilling and/or aquifer testing in this area. The field and data interpretation methods used in this study were successfully applied to the complex subsurface environment and "single-well" test setting in northwest Boise, and can be applied more generally in the lower Boise River valley where the needs to characterize the subsurface and to analyze single-well tests for hydraulic parameters and the interaction of units and structures are commonly encountered.

RECOMMENDATIONS

1. It has been shown that high-resolution shallow seismic reflection data can provide subsurface images of hydrologically important strata and environments in the region used by water wells in the lower Boise River valley. Calibration of the seismic reflection images with lithologic and geophysical logs at one or several adjacent deep wells, especially wells with construction data and which have been or could be used in aquifer tests, would better constrain interpretations of sedimentary environments in the subsurface, and provide constraints on the composition and lateral

and vertical distribution of hydrostratigraphic units that are important for explaining drawdown behavior in wells.

2. Objective means for correlating sand units in wells are needed. Availability of lithologic data on samples collected during drilling (grain composition, shape, size distribution...) and/or of samples from a repository for non-destructive analysis would be valuable for sand unit correlation. Similarly, general access to borehole geophysical logs for wells in the valley would be quite valuable.

3. The seismic section produced for this study was oriented perpendicular to structure but parallel to the strike of primary sedimentological features (such as prograding delta fronts). A seismic section oriented perpendicular to the section presented here would give a complementary structural/sedimentological view of the subsurface in the area of the WIFG and thereby would provide valuable detail on sedimentary environments and their internal composition and geometry that are significant for understanding ground-water flow and well hydraulics.

4. Surface sources, such as the EWG sources used in this study, provide adequate source strength while not being limited by difficult drilling conditions or landowner apprehension regarding drilling. Although the truck-mounted EWG I did not provide sufficient energy in coarse deposits directly adjacent to the Boise River channel, it probably would be sufficient for data collected away from the river in areas with more consistent fine-grained sediments at the surface (i.e., on the benches). We recommend trying EWG and/or vibrator sources in more urbanized areas (where they are likely to provide sufficient energy with a minimum of surface and environmental disturbance) to determine if high-quality images can be acquired, and if so, to determine appropriate acquisition configuration and parameters.

5. Unlined irrigation canals should provide opportunities for extended seismic traverses in heavily urbanized areas, during the irrigation off season.

6. Future aquifer testing in the area, and the lower Boise River valley in general, should be run for periods long enough to register responses from observation wells within reasonable lateral or vertical distances of the pumping well; preliminary modeling can provide estimates of what such times and distances might be. And, detailed well construction information and step tests with detailed records of flow rates, elapsed time and drawdown/recovery are invaluable in demonstrating whether a pumping test can be analyzed without corrections at the pumping well (i.e., whether well losses influence drawdown responses in the well), and if not, what corrections should be made.

7. We recommend that the model presented here be tested against additional information if new seismic lines or wells and aquifer tests in the area provide the opportunity to refine model inputs and/or run the model with additional wells and, hopefully, responses at monitor wells.

ACKNOWLDEGMENTS

Research reported here was supported in part by grant 684-K102 from the Idaho Water Resources Research Institute and by the Idaho State Board of Education Higher Education Research Council.

Access to the Western Idaho Fairgrounds and the Settlers canal is greatly appreciated. Dr. Gerry Schuster of the University of Utah allowed us use of the Bison EWG III. Well data were provided by Boise City, Boise School District, Capitol Securities Water Corporation, Garden City, Scanlan Engineering, U.S. Geological Survey and United Water Idaho. Robert J. Vincent contributed significantly to the seismic data acquisition and processing. Dr. Spencer H. Wood provided insight into interpretation of seismic data. Students who assisted in several phases of this project are Susan Kay, Bill Hudson, R.D. Bolger, William Bennecke, Phil Galloway and Loren Pearson. Boise State University Center for Geophysical Investigation of the Shallow Subsurface Technical Report 95-17.

REFERENCES CITED

Barrash, W. and Dougherty, M.E., 1995, Accurate simulation of axisymmetric and non-symmetric flow to a well with MODFLOW (abs.): Geological Society of America Abstracts with Programs, v. 27, no. 6, p. A-187.

Barrash, W. and Ralston, D., 1991, Analytical modeling of a fracture zone in the Brule formation as an aquifer receiving leakage from water-table and elastic aquitards: Journal of Hydrology, v. 125, p. 1-24.

Berg, O.R., 1982, Seismic detection and evaluation of delta and turbidite sequences: Their application to exploration for the subtle trap: American Association of Petroleum Geologists Bulletin, v. 66, no. 9, p. 1271-1288.

Brown, L.F., Jr. and Fisher, W.L., 1977, Seismic stratigraphic interpretation of depositional systems: Examples from Brazilian rift and pull-apart basins, in Payton, C.E., ed., Seismic stratigraphy - applications to hydrocarbon exploration: American Association of Petroleum Geologists Memoir 26, p. 213-248.

Cant, D.J., 1982, Fluvial facies models and their application, in Scholle, P.A. and Spearing, D., eds., Sandstone depositional environments: American Association of Petroleum Geologists Memoir 31, p. 115-137.

Changsong, L., Qi, Y., and Sitian, L., 1991, Structural and depositional patterns in the Tertiary Baise Basin, Guang Xi Autonomous Region (southeastern China): a predictive model for fossil fuel exploration, in Anadon, P., Cabrera, Ll. and Kelts, K., eds., Lacustrine facies analysis: International Association of Sedimentologists Special Publication 13, p. 75-92.

Coleman, J.M. and Prior, D.B., 1982, Deltaic environments of deposition, in Scholle, P.A. and Spearing, D., eds., Sandstone depositional environments: American Association of Petroleum Geologists Memoir 31, p. 139-178.

Cooper, H.H., Jr. and Jacob, C.E., 1946, A generalized graphical method for evaluating formation constants and summarizing well-field history: Transactions, American Geophysical Union, v. 27, no. IV, p. 526-534.

Dougherty, M.E., Vincent, R.J., and Barrash, W., 1995, Seismic reflection tests at the Western Idaho Fairgrounds, Ada County, Idaho: unpublished Technical Report BSU CGISS 95-19, Center for Geophysical Investigation of the Shallow Subsurface, Boise State University, Boise, Idaho, 70 p.

Driscoll, F.G., 1986, Groundwater and wells, 2nd ed.: Johnson Division, St. Paul, MN, 1089 p.

Fogg, G.E., 1989, Stochastic analysis of aquifer interconnectedness: Wilcox Group, Trawick area, east Texas: Texas Bureau of Economic Geology, Report of Investigations no. 189, 68 p.

Freeze, R.A. and Cherry, J.A., 1979, Groundwater: Prentice-Hall, Inc., Englewood Cliffs, NJ, 604 p.

Hantush, M.S., 1964, Hydraulics of wells: Advances in Hydroscience, 1, p. 281-432.

Kimmel, P.G., 1982, Stratigraphy, age, and tectonic setting of the Miocene-Pliocene lacustrine sediments of the western Snake River Plain, Oregon and Idaho, in B. Bonnichsen and R.M. Breckenridge, eds., Cenozoic Geology of Idaho: Idaho Geological Survey Bulletin 26, p. 559-578.

Malde, H.E., 1972, Stratigraphy of the Glenns Ferry Formation from Hammett to Hagerman, Idaho: U.S. Geological Survey Bulletin 1331-D, p. D1-D19.

Malde, H.E. and Powers, H.A., 1962, Upper Cenozoic stratigraphy of the western Snake River Plain, Idaho: Geological Society of America Bulletin, v. 73, p. 1197-1220.

McDonald, M.G. and Harbaugh, A.W., 1988, A modular three-dimensional finite-difference ground-water flow model: Techniques of Water-Resources Investigations of the U.S. Geological Survey, Book 6, Chapter A1.

Middleton, L.T., Porter, M.L., and Kimmel, P.G., 1985, Depositional settings of the Chalk Hills and Glenns Ferry formations west of Bruneau, Idaho, in R.M. Flores and S.S. Kaplan, eds, Cenozoic paleogeography of the west-central United States: Rocky Mountain Section, Society of Economic Paleontologists and Mineralogists, p. 37-53.

Mills, D.E. , 1991, Testing of the new Goddard well: Report to Boise Water Corporation by J.M. Montgomery Consulting Engineers, Boise, ID.

Mitchum, R.M., Jr., Vail, P.R. and Sangree, J.B., 1977, Seismic stratigraphy and global changes of sea level, Part 6: Stratigraphic interpretation of seismic reflection patterns in depositional sequences, in Payton, C.E., ed., Seismic stratigraphy - applications to hydrocarbon exploration: American Association of Petroleum Geologists Memoir 26, p. 117-133.

Morisawa, M., 1985, Rivers, form and process: Longman Group Ltd., New York, 222 p.

Newton, G.D., 1991, Geohydrology of the regional aquifer system, western Snake River Plain, southwestern Idaho: U.S. Geological Survey Professional Paper 1408-G, 52 p.

Othberg, K.L., 1994, Geology and geomorphology of the Boise Valley and adjoining areas, western Snake River Plain, Idaho: Idaho Geological Survey Bulletin 29, 54 p.

Scott, D.L., Ng'ang'a, P., Johnson, T.C. and Rosendahl, B.R., 1991, High-resolution acoustic character of Lake Malawi (Nyasa), East Africa and its relationship to sedimentary processes, in, Anadon, P., Cabrera, Ll. and Kelts, K., eds., Lacustrine facies analysis: International Association of Sedimentologists Special Publication 13, p. 129-145.

Smith, G.R., Swyridczuk, K., Kimmel, P.G., and Wilkinson, B.H., 1982, Fish biostratigraphy of late Miocene to Pleistocene sediments of the western Snake River Plain, Idaho: in, B. Bonnichsen and R.M. Breckenridge, eds., Cenozoic Geology of Idaho: Idaho Geological Survey Bulletin 26, p. 519-541.

Squires, E., Osiensky, J.L., and Wood, S.H., 1992, Hydrogeologic framework of the Boise aquifer system, Ada County, Idaho: Idaho Water Resources Research Institute, Research Technical Report 14-08-0001-G1559-06, Moscow, ID, 75 p.

Squires, E., Wood, S.H., Osiensky, J.L., and Dittus, R.D., 1993, Groundwater conditions and hydraulic testing of the Boise-Fan aquifer of southeast Boise River valley, Ada County, Idaho: Report to Boise Water Corporation, Boise, Idaho.

U.S. Environmental Protection Agency, 1975, Manual of water well construction practices: EPA-570/9-75-001, U.S. EPA Water Supply Division, Washington, D.C., 156 p.

Walker, R.G., 1979, Facies models, 8. Turbidites and associated coarse clastic deposits, in Walker, R.G., ed., Facies Models, Geoscience Canada Reprint Series 1, p. 91-103.

Walker, R.G. and Cant, D.J., 1979, Facies models, 3. Sandy fluvial systems, in Walker, R.G., ed., Facies Models, Geoscience Canada Reprint Series 1, p. 23-31.

Wood, S.H., 1994, Seismic expression and geological significance of a lacustrine delta in Neogene deposits of the western Snake River Plain, Idaho: American Association of Petroleum Geologists Bulletin, v. 78, no. 1, p. 102-121.

Wood, S.H. and Anderson, J.E., 1981, Geology, in Mitchell, J.C., ed., Geothermal Investigations in Idaho, Part 11, Geological, hydrological, geochemical, and geophysical investigations of the Nampa-Caldwell and adjacent areas, southwestern Idaho: Idaho Department of Water Resources, Water Information Bulletin 30, p. 9-31.

Table 1. Step test data for elapsed time intervals of 50±1.5 min per step, after Mills (1991).

Step (i)	Q_i: Discharge Rate, gpm	Time during step, min	s_i: Drawdown during step, ft	Q_i/s_i: Specific capacity gpm/ft	s_i/Q_i ft/gpm
1	350?*	50**	25**	14	0.071
2	600	51.5	37.09	16.2	0.062
3	1000	48.8	66.67	15	0.067
4	1300	50	84.96	15.3	0.065
5	1500	50.5***	99.68***	15	0.066
6	1714	50****	105.5****	16.2	0.062

* estimated rate - discharge was below minimum calibrated rate of flowmeter
** extrapolated from trend through 12.5 minutes and 24.78 ft drawdown
*** interpolated from drawdowns at 47.1 and 54.9 minutes elapsed time in step 5
**** interpolated from drawdowns at 47.5 and 57 minutes elapsed time during constant-rate pumping test

Table 2. Drawdown data for Goddard2 well constant-rate pumping test, taken directly from Mills, 1991.

BWC - GODDARD ST. CONSTANT RATE DRAWDOWN TEST
TESTING BY LAYNE OF IDAHO, INC.
PUMP ON: 2/28/91 @ 8:00:00
PUMP OFF: 2/28/91 @ 16:00:00
(DRAWDOWN FOR 255.5 MIN)
METHOD OF FLOW MEASUREMENT: 8" ORIFICE
METHOD OF WATER LEVEL MEASUREMENT: ELECTRIC WIRELINE SOUNDER
PUMP AT 200'
STATIC WATER LEVEL (ft) 44.47' (TOC)
AVERAGE FLOW RATE APPROXIMATELY 1714 gpm

DRAWDOWN DATA

DATE	ACTUAL TIME	ELAPSED TIME (MIN)	DTW (ft)	DRAWDOWN (ft)	COMMENTS
2/28/91	8:00:00	0.00	44.47	0.00	meas. top of case
	8:01:45	1.75	138.85	94.38	
	8:04:00	4.00	141.14	96.67	
	8:04:30	4.50	142.05	97.58	1750 gpm
	8:07:30	7.50	143.65	99.18	
	8:12:00	12.00	144.82	100.35	sounder hung up
	8:13:00	13.00	144.88	100.41	
	8:14:00	14.00	145.18	100.71	
	8:15:00	15.00	145.27	100.80	
	8:16:00	16.00	145.51	101.04	
	8:17:00	17.00	145.67	101.20	
	8:18:00	18.00	145.87	101.40	
	8:20:00	20.00	146.13	101.66	
	8:25:30	25.50	146.72	102.25	
	8:34:00	34.00	148.88	104.41	1711 gpm/rpm =1425
	8:47:30	47.50	149.85	105.38	
	8:57:00	57.00	150.45	105.98	
	9:06:00	66.00	151.09	106.62	
	9:15:00	75.00	154.17	109.70	adj. Q=1711 ,inc. rpm
	9:25:00	85.00	154.74	110.27	
	9:35:00	95.00	155.26	110.79	
	9:48:00	108.00	155.77	111.30	Q=1715
	10:05:00	125.00	156.49	112.02	
	10:27:00	147.00	156.85	112.38	
	10:45:00	165.00	157.40	112.93	adj. Q=1711, inc. rpm to 1450
	11:08:00	188.00	158.57	114.10	inc. rpm to 1475 Q=1720
	11:09:00	189.00	159.45	114.98	
	11:32:00	212.00	160.02	115.55	Q=1710, rpm=1450
	11:51:00	231.00	160.61	116.14	Q=1710, rpm=1475
	12:15:00	255.00	160.94	116.47	inc. Q=1710, rpm=1475
	12:45:00	285.00	162.61	118.14	
	13:12:00	312.00	163.80	119.33	at 13:00, inc Q to 1720 gpm, rpm=1475
	13:45:00	345.00	164.52	120.05	Q=1745
	14:15:00	375.00	165.75	121.28	at 13:55, inc Q to 1720 gpm, up from 1700
	14:45:00	405.00	166.52	122.05	at 14:43
	15:17:00	437.00	166.94	122.47	Q=1710 steady
	15:45:00	465.00	168.05	123.58	inc Q from 1700 to 1715 gpm, rpm=1475 at 15:30
	15:59:00	479.00	168.21	123.74	at 15:50, Q=1710 Temp 62°F

Table 3. Values of t_c for ranges of distances to boundaries and for storage values, where t_c is time at which $u \leq 0.01$, r_b is distance from Goddard2 well to the boundary, r_i is distance from Goddard2 well to the image well, S_s is specific storage of the aquifer, and S is storativity of the aquifer using S_s and 100 ft for aquifer thickness.

	$S_s = 10^{-4}$ ft^{-1}; $S = 10^{-2}$	$S_s = 10^{-5}$ ft^{-1}; $S = 10^{-3}$	$S_s = 10^{-6}$ ft^{-1}; $S = 10^{-4}$
r_b=50 ft; r_i=100 ft	t_c = 694 min	t_c = 69.4 min	t_c = 6.94 min
r_b=250 ft; r_i=500 ft	$t_c = 1.74 \times 10^4$ min	t_c = 1740 min	t_c = 174 min
r_b=500 ft; r_i=1000 ft	$t_c = 6.94 \times 10^4$ min	t_c = 6940 min	t_c = 694 min
r_b=1000 ft; r_i=2000 ft	$t_c = 2.78 \times 10^5$ min	$t_c = 2.78 \times 10^4$ min	t_c = 2780 min
r_b=2500 ft; r_i=5000 ft	$t_c = 1.74 \times 10^6$ min	$t_c = 1.74 \times 10^5$ min	$t_c = 1.74 \times 10^4$ min
r_b=5000 ft; r_i=10000 ft	$t_c = 6.94 \times 10^6$ min	$t_c = 6.94 \times 10^5$ min	$t_c = 6.94 \times 10^4$ min

Table 4. Model grid dimensions.

Row/Col	Row Width (ft)	Col Width (ft)	Row/Col	Row Width (ft)	Col Width (ft)
1	141.9	9222	26	.008215	16.04
2	117.8	9222	27	.005513	10.76
3	79.05	9222	28	.0037	7.224
4	53.05	9222	29	.002483	4.848
5	35.61	9222	30	.0016667	3.254
6	23.9	9222	31	.833333 (well)	2.184
7	16.04	9222	32	.0016667	1.466
8	10.76	9222	33	.002483	.9836
9	7.224	9222	34	.0037	.6602
10	4.848	5000	35	.005513	.4431
11	3.254	2500	36	.008215	.2974
12	2.184	1250	37	.01224	.1996
13	1.466	750	38	.01824	.1339
14	.9836	500	39	.02717	.08989
15	.6602	500	40	.04049	.06033
16	.4431	735	41	.06033	.04049
17	.2974	580.5	42	.08989	.02717
18	.1996	389.6	43	.1339	.01824
19	.1339	261.5	44	.1996	.01224
20	.08989	175.5	45	.4431	.008215
21	.06033	117.8	46	.4431	.005513
22	.04049	79.05	47	.6022	.0037
23	.02717	53.05	48	.9836	.002483
24	.01824	35.61	49	1.466	.0016667
25	.01224	23.9	50	2.184	.833333 (well)

Table 4 continued. Model grid dimensions.

Row/Col	Row Width (ft)	Col Width (ft)	Row/Col	Row Width (ft)	Col Width (ft)
51	3.254	.0016667	76	8667	35.61
52	4.848	.002483	77	8667	53.05
53	7.274	.0037	78	8667	79.05
54	10.76	.005513	79	8667	117.8
55	16.04	.008215	80	8667	175.5
56	23.9	.01224	81		261.5
57	35.61	.01824	82		389.6
58	53.05	.02717	83		580.5
59	79.05	.04049	84		855
60	117.8	.06033	85		1289
61	175.5	.08989	86		1920
62	246.5	.1339	87		2861
63	220	.1996	88		4236
64	350	.4431	89		4036
65	550	.4431	90		4000
66	700	.6022	91		6000
67	1000	.9836	92		8625
68	1500	1.466	93		8625
69	2500	2.184	94		8625
70	4000	3.254	95		8625
71	6500	4.848	96		8625
72	8667	7.274	97		8625
73	8667	10.76	98		8625
74	8667	16.04	99		8625
75	8667	23.9			

Table 5. Model layer dimensions.

Unit	Layer Number	Layer Thickness (ft)	Layer Bottom (ft)
Aquitard	1	66.5	-66.5
Aquitard	2	100	-166.5
Aquitard	3	50	-216.5
Aquitard	4	30	-246.5
Aquitard	5	21	-267.5
Aquitard	6	13.5	-281
Aquitard	7	9	-290
Aquitard	8	6	-296
Aquitard	9	4	-300
Aquifer	10	4.21	-304.21
Aquifer	11	6.32	-310.53
Aquifer	12	9.47	-320
Aquifer	13	17.5	-337.5
Aquifer	14	17.5	-355
Aquifer	15	9.47	-364.47

Table 5 continued. Model layer dimensions.

Unit	Layer Number	Layer Thickness (ft)	Layer Bottom (ft)
Aquifer	16	6.32	-370.79
Aquifer	17	4.21	-375
Aquifer	18	4.5	-379.5
Aquifer	19	8	-387.5
Aquifer	20	8	-395.5
Aquifer	21	4.5	-400
Aquitard	22	4	-404
Aquitard	23	6	-410
Aquitard	24	9	-419
Aquitard	25	13.5	-432.5
Aquitard	26	21	-453.5
Aquitard	27	30	-485.5
Aquitard	28	50	-535.5
Aquitard	29	100	-635.5
Aquitard	30	66.5	-700

Table 6. Time discretization in MODFLOW simulation of Goddard2 pumping test.

Period	PERLEN* (min)	NSTP**	TSMULT***
1	1	30	1.2
2	10	30	1.2
3	100	30	1.2
4	450	25	1.2

* PERLEN is the length of a given period
** NSTP is the number of time steps in a given period
*** TSMULT is the multiplier for successive time steps within a given period

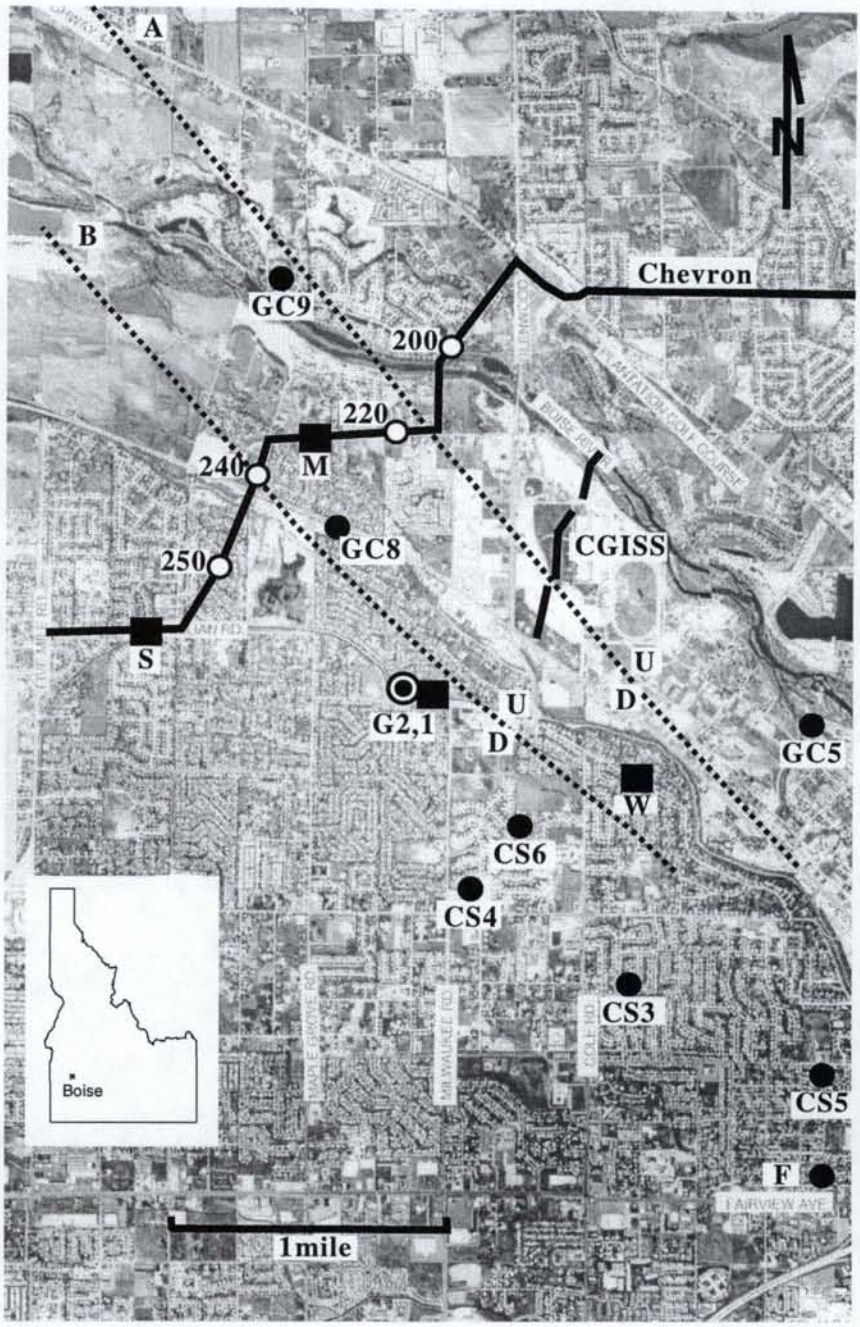

Figure 1. Study area in northwest Boise, Idaho showing wells, seismic lines (Chevron IB–2 and CGISS), and projected surface traces of faults A (Eagle–West Boise fault of Squires et al., 1992) and B (Wood, unpublished data) with relative up and down displacement labeled U and D, respectively. Numbered circles on Chevron line are shot points. A double circle identifies the Goddard2 well (G2) pumped for the test analyzed in this report; black squares are observation wells for that test (G1 is Goddard1 well, W is Westmoreland, S is Settlers, M is Millstream). Black circles are deep wells for stratigraphic interpretation (CS3, CS4, CS5, CS6 are Capitol Securities wells; GC5, GC8, GC9 are Garden City wells; F is United Water Idaho's Fisk well).

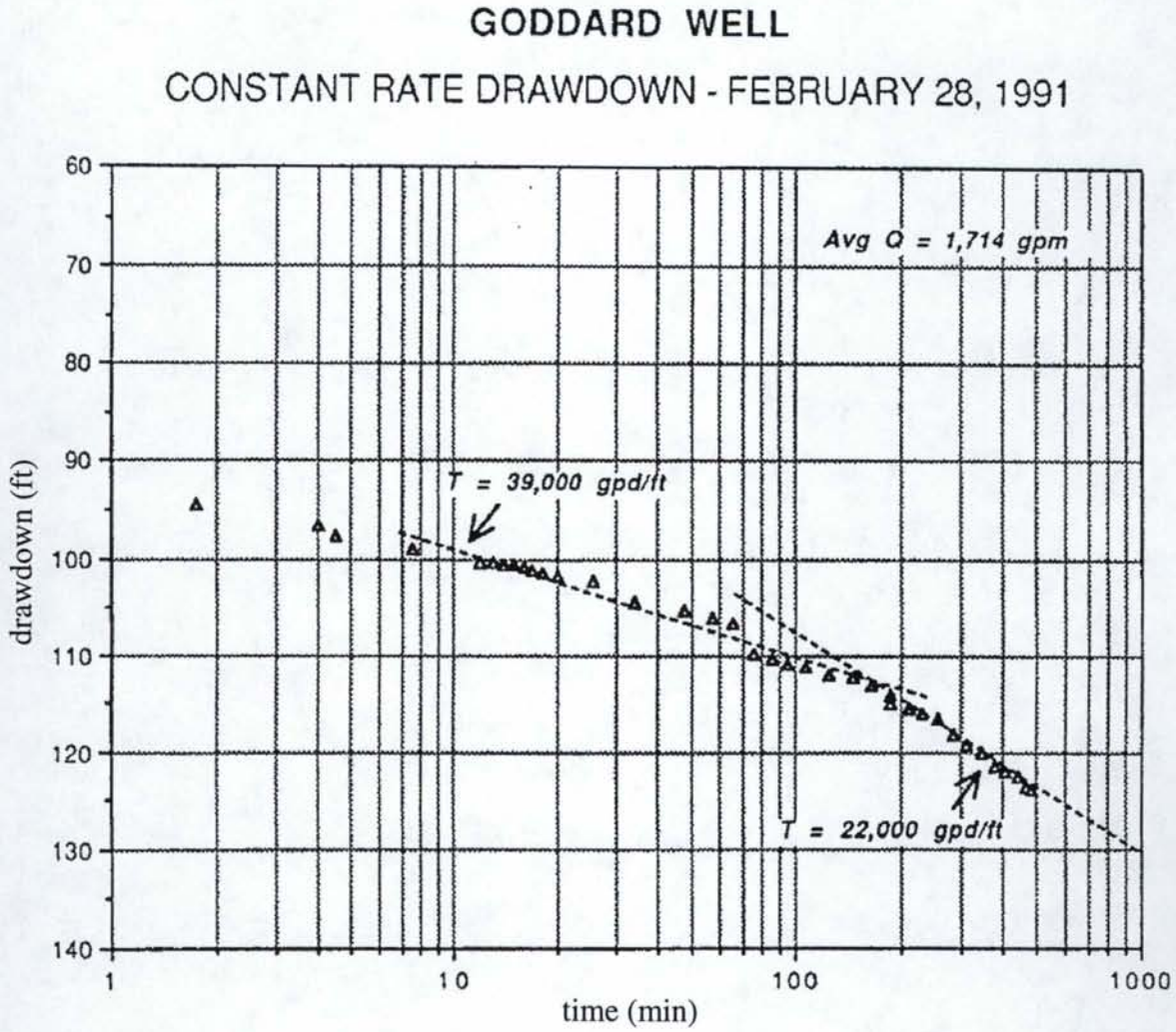

Figure 2. Semilog plot of drawdown vs time for pumping test at the Goddard2 well. From Mills, 1991.

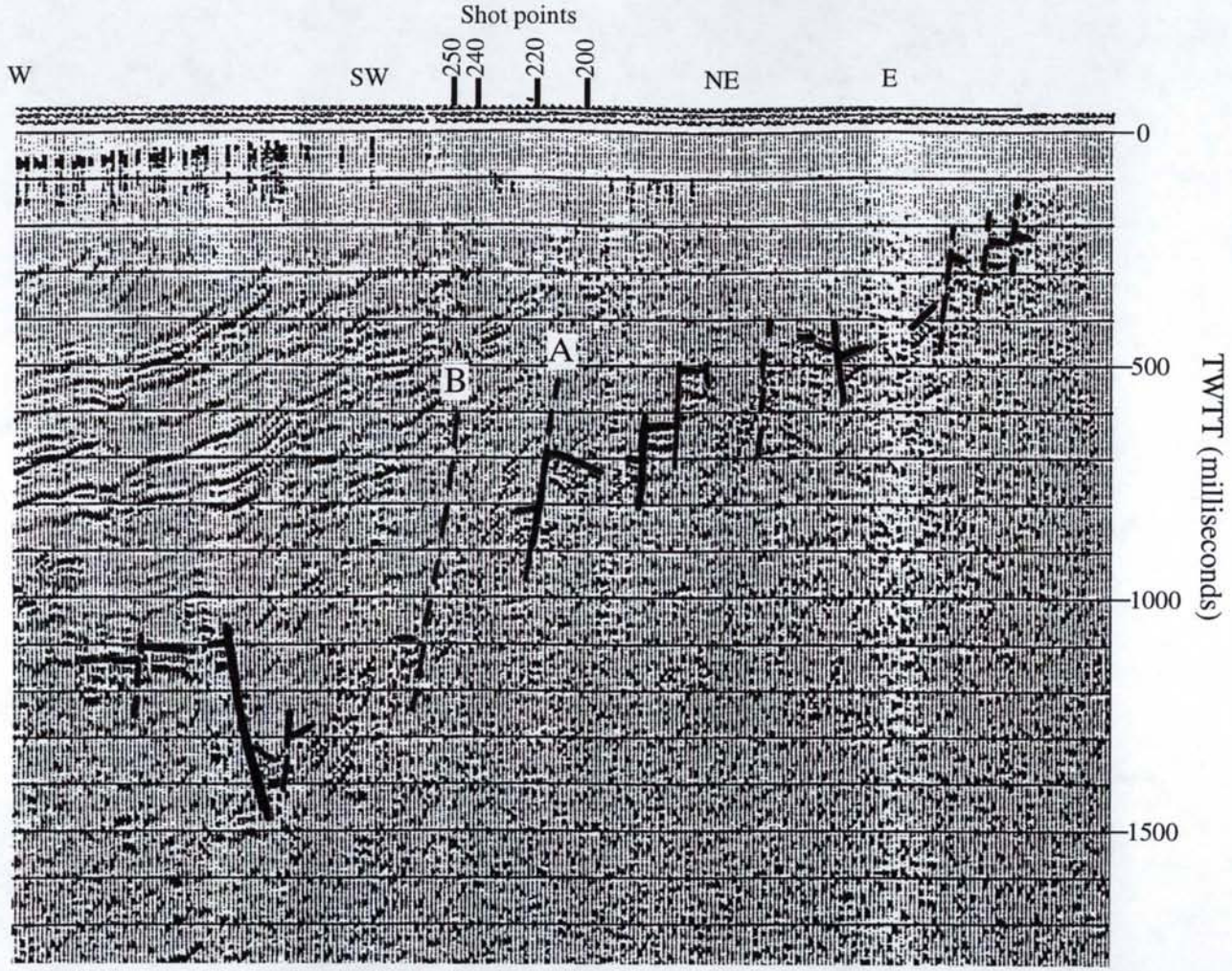

Figure 3. Segment of Chevron IB-2 seismic line with shot points for reference (see Figure 1) and locations for faults A (Eagle-West Boise fault) and B (unnamed fault). Seismic imaging not captured above 250-300 msec TWTT (two-way travel time). Reflector at top of basalt is enhanced in this figure; basinward-dipping reflectors above likely represent sand bodies in deep- water fine grained lacustrine sediments.

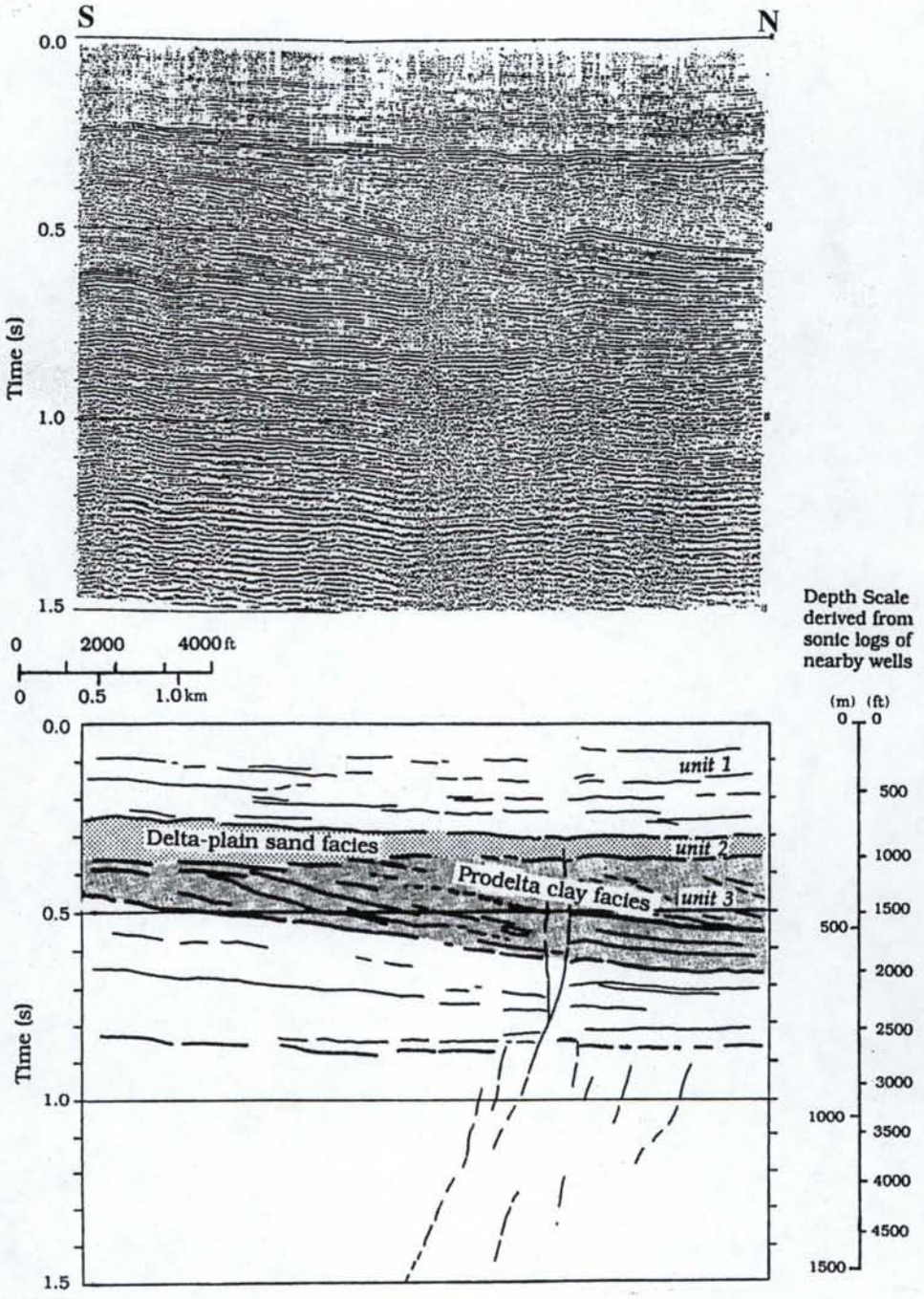

Figure 4. Subaerial and lacustrine sedimentary environments identified with deep seismic reflection profiles near Caldwell, Idaho (approximately 25 miles west of Boise) illustrate the relevance of seismic data to subsurface investigations in the western Snake River Plain After Wood, 1994, Figure 6, reprinted by permission of the American Association of Petroleum Geologists Bulletin.

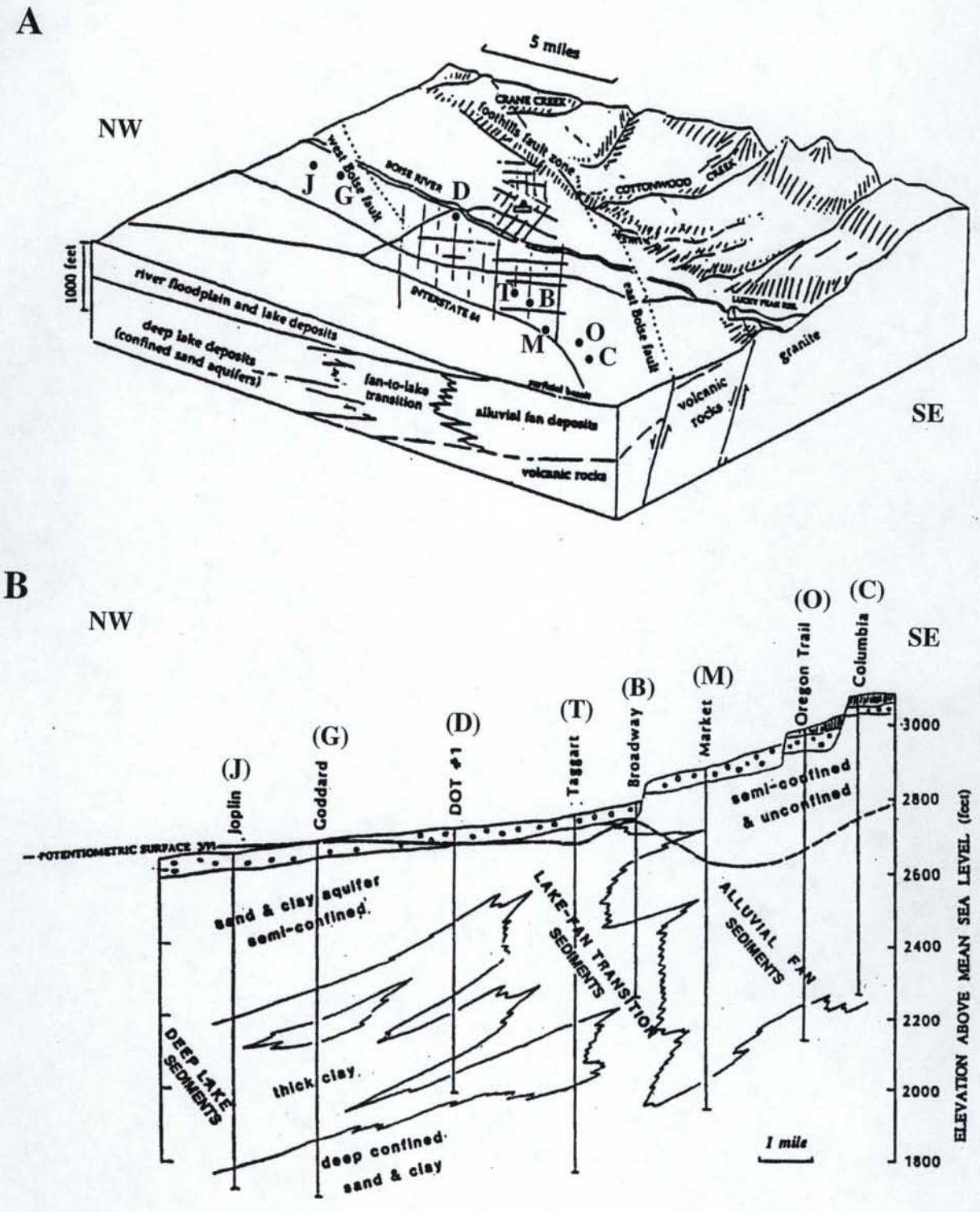

Figure 5. Schematic block diagram (A) and cross section (B) after Squires et al. (1992) showing interpreted distributions of sedimentary environments in the Boise area and location of the Goddard1 well.

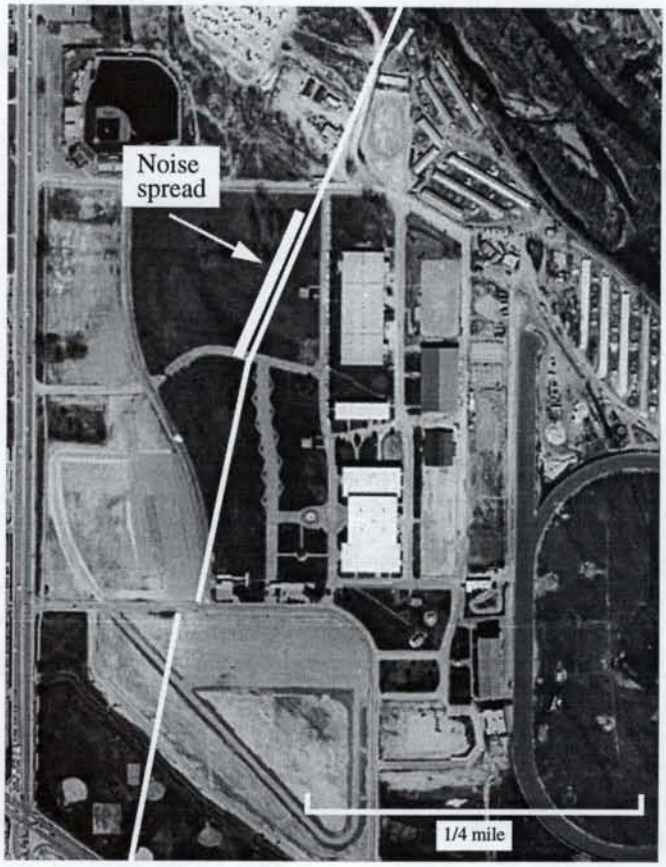

Figure 6. Location of CGISS seismic line and noise spread at the Western Idaho Fairgrounds. Glenwood Avenue is at the left side of the photograph. Offsets in seismic line were necessary to avoid extended lengths of asphalt along the line.

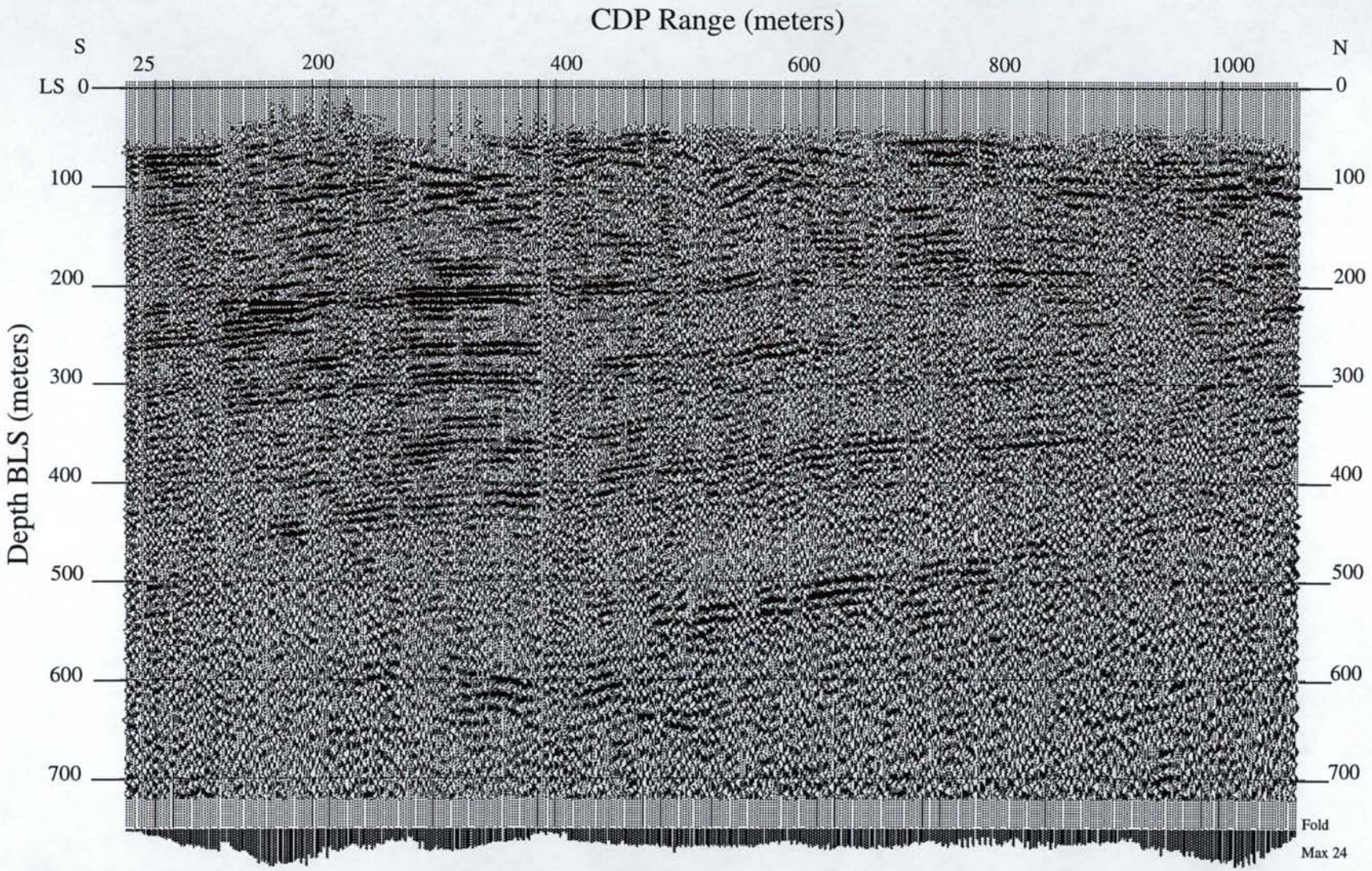

Figure 7A. CGISS high-resolution seismic reflection profile run at the Western Idaho Fairgrounds using the EWG III source. Length reference across the profile is the CDP (Common Depth Point) Range, given in meters. LS is land surface (datum) which is relatively flat along the profile. Line is oriented at a high angle to faults and subparallel to the direction of sediment influx to the basin.

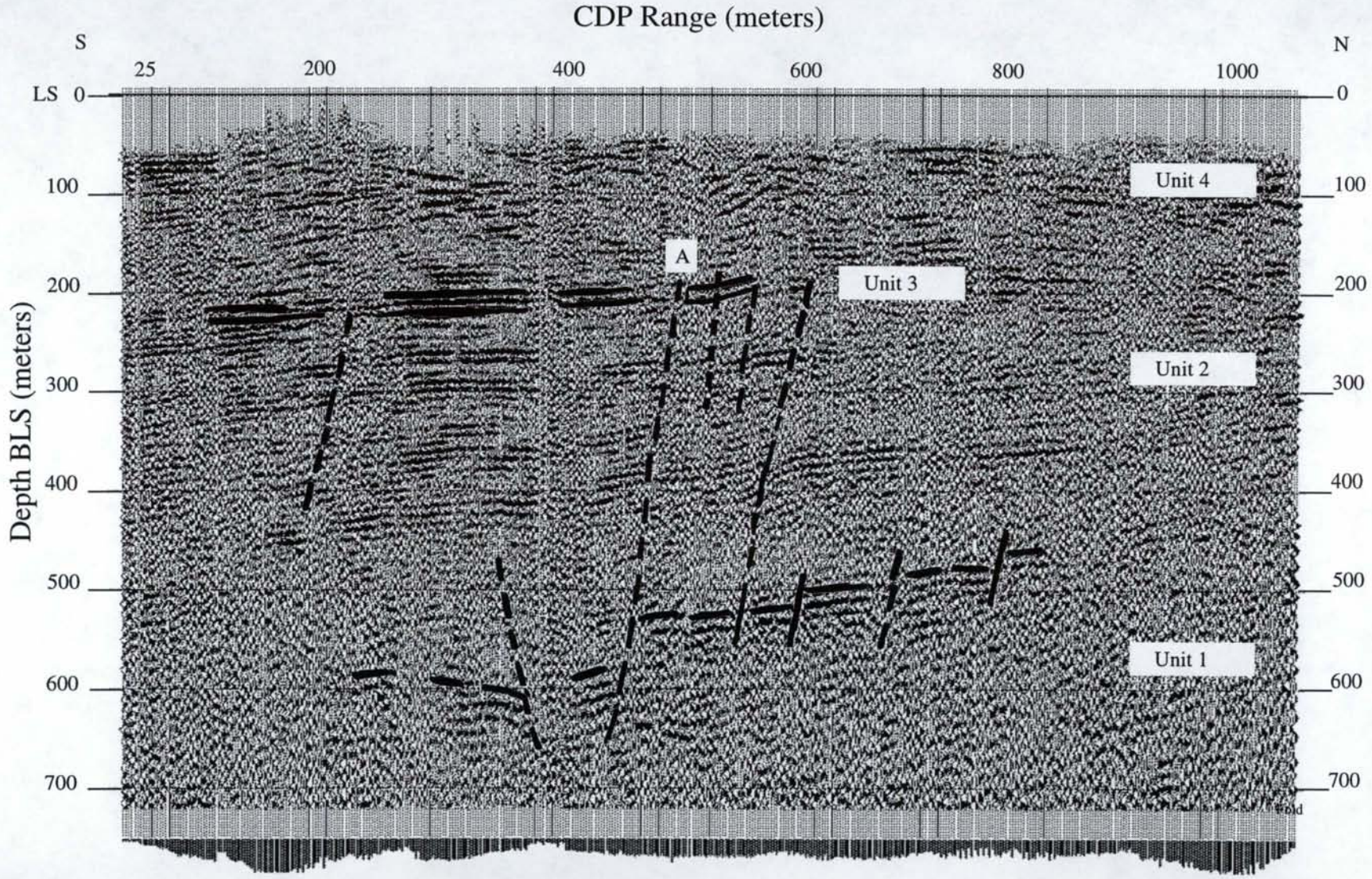

Figure 7B. Seismic stratigraphic units and faults interpreted from CGISS seismic line. The tops of seismic stratigraphic units 1, 2 and 3 are highlighted. A is Eagle-West Boise fault.

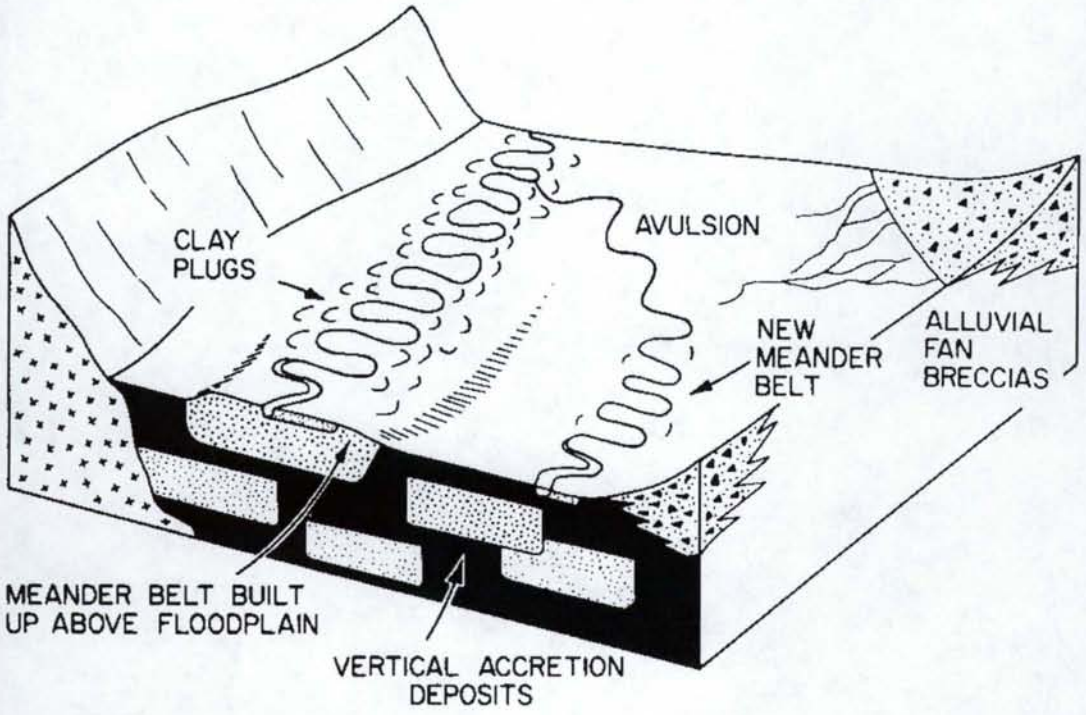

Figure 8. Schematic diagram of floodplain environment showing linear sand stringers surrounded by fine-grained vertical accretion deposits. From Walker and Cant, 1979, Figure 8A, reprinted by permission of the Geological Association of Canada.

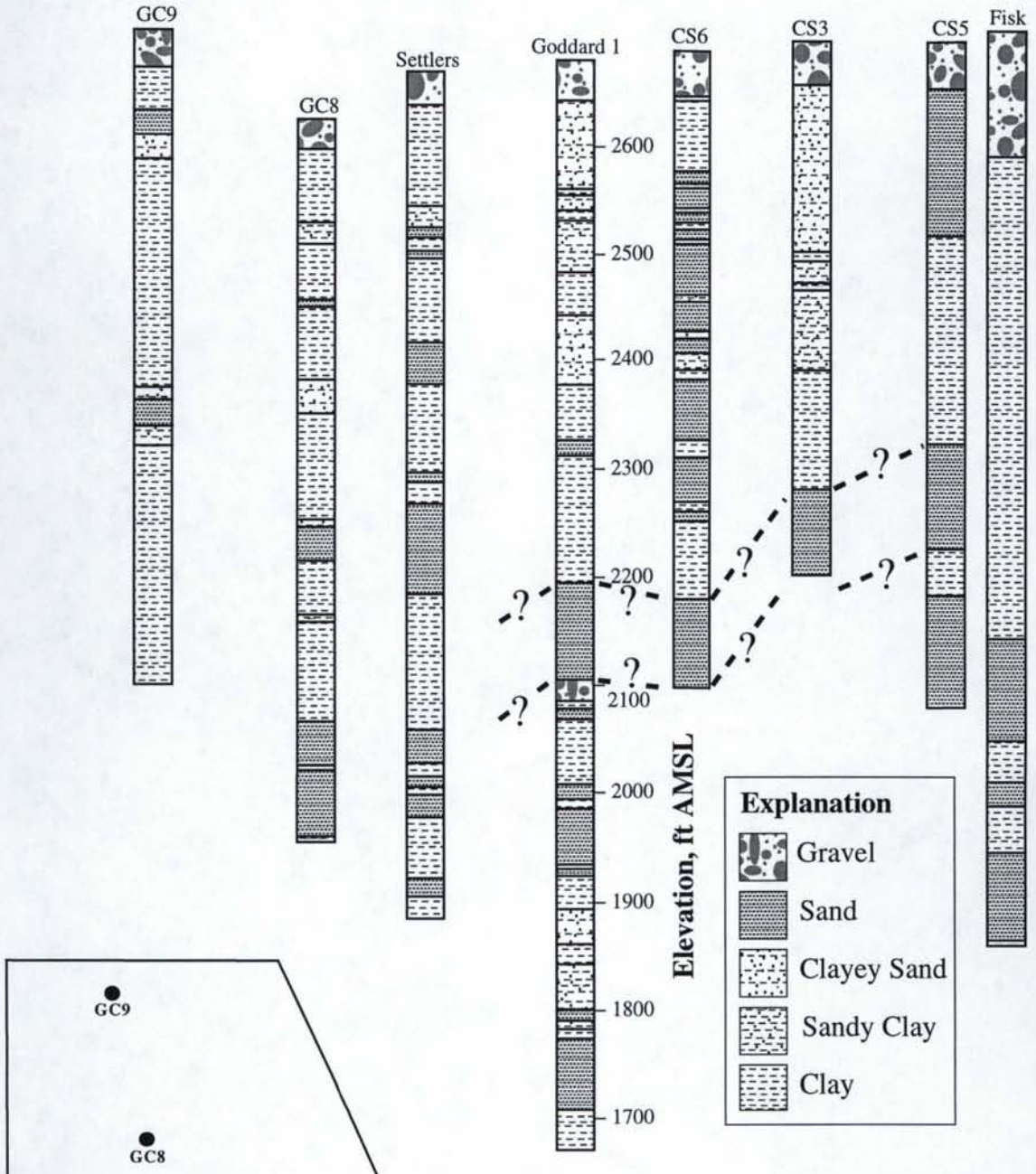

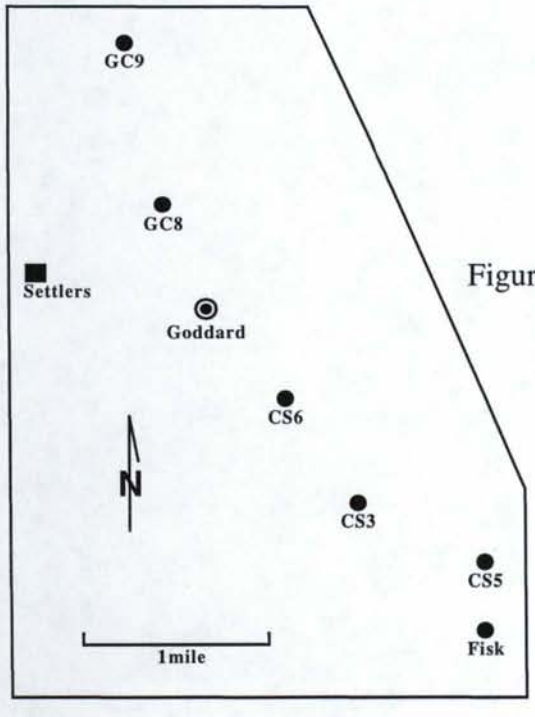

Figure 9. Lithologic logs of deep wells, including Goddard1 well, located along an orientation parallel to likely direction of sediment influx. Thick sand and thick fine–grained units are common. Sand units are tentatively correlated with the Goddard2 producing zone based on comparable thicknesses and consistency with a stream gradient in the permissible range for a meandering stream. See Figure 1 for locations relative to features in northwest Boise.

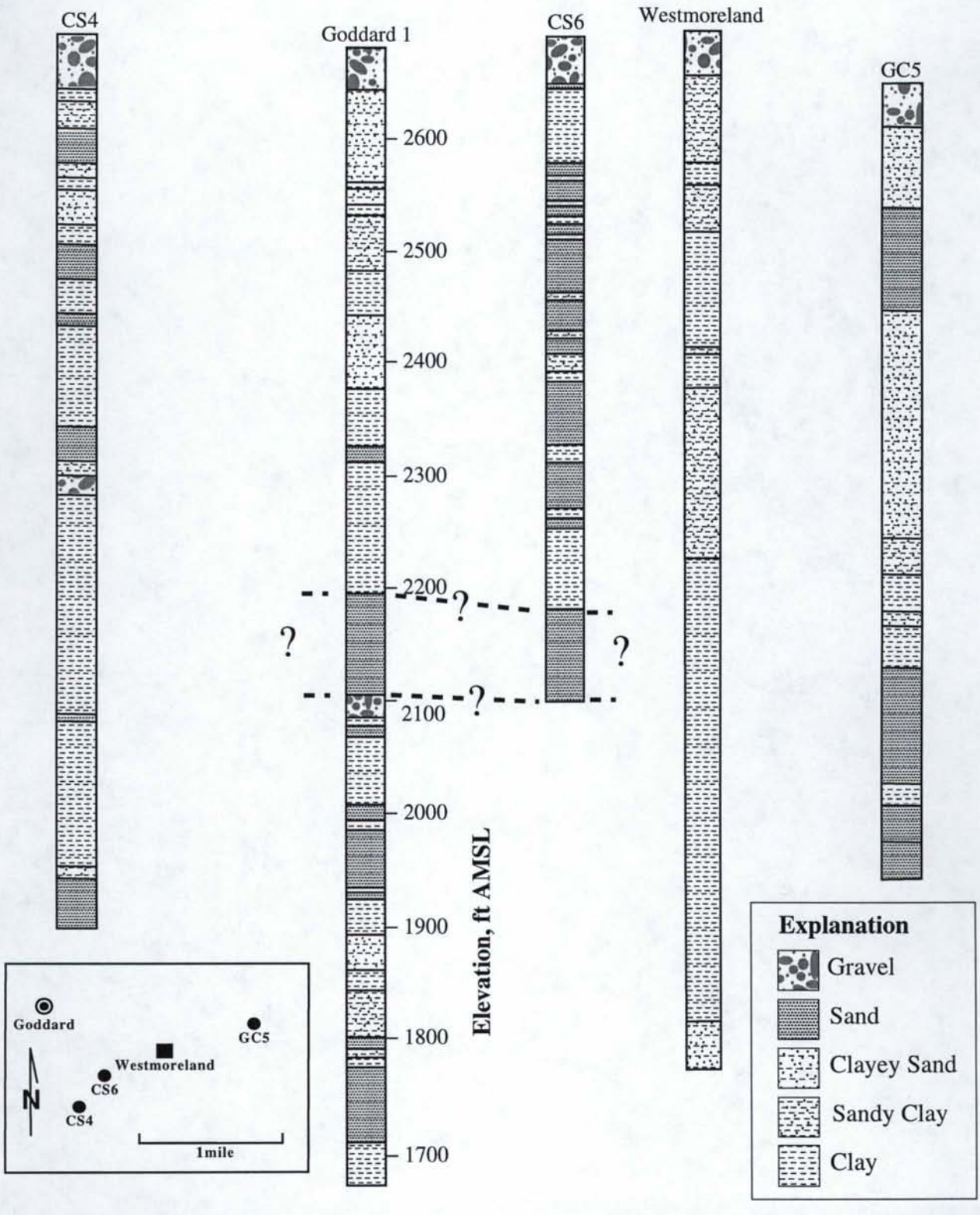

Figure 10. Lithologic logs of deep wells, including Goddard1 well, located along an orientation at a high angle to likely direction of sediment influx. The thick sand in the Goddard1 well at about 2100–2200 ft elevation might be correlated with sand in similar position in CS6, but other deep wells in the area do not have a similar unit in a similar position. See Figure 1 for locations relative to features in northwest Boise.

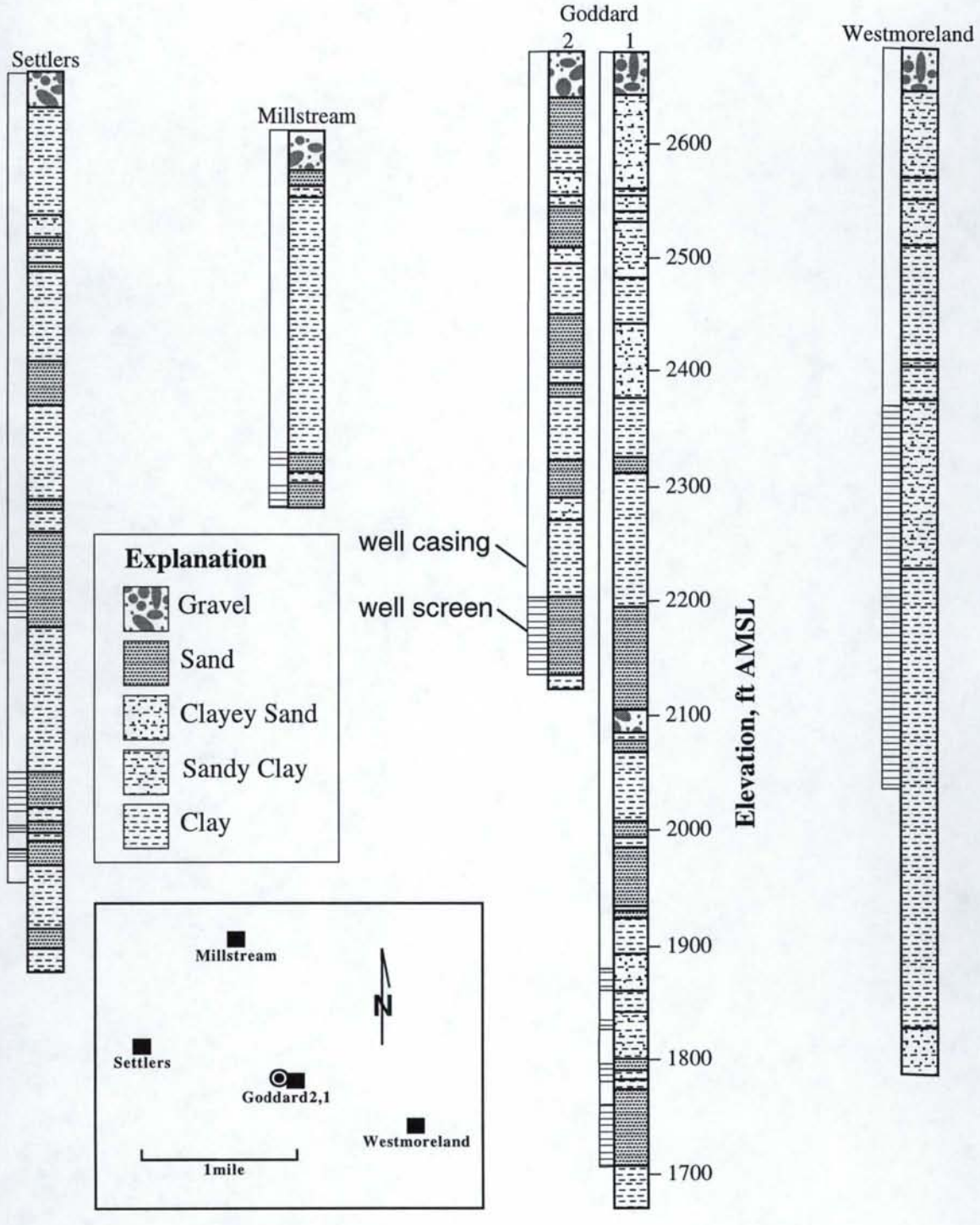

Figure 11. Well construction and lithologic logs for wells monitored during the Goddard2 pumping test.

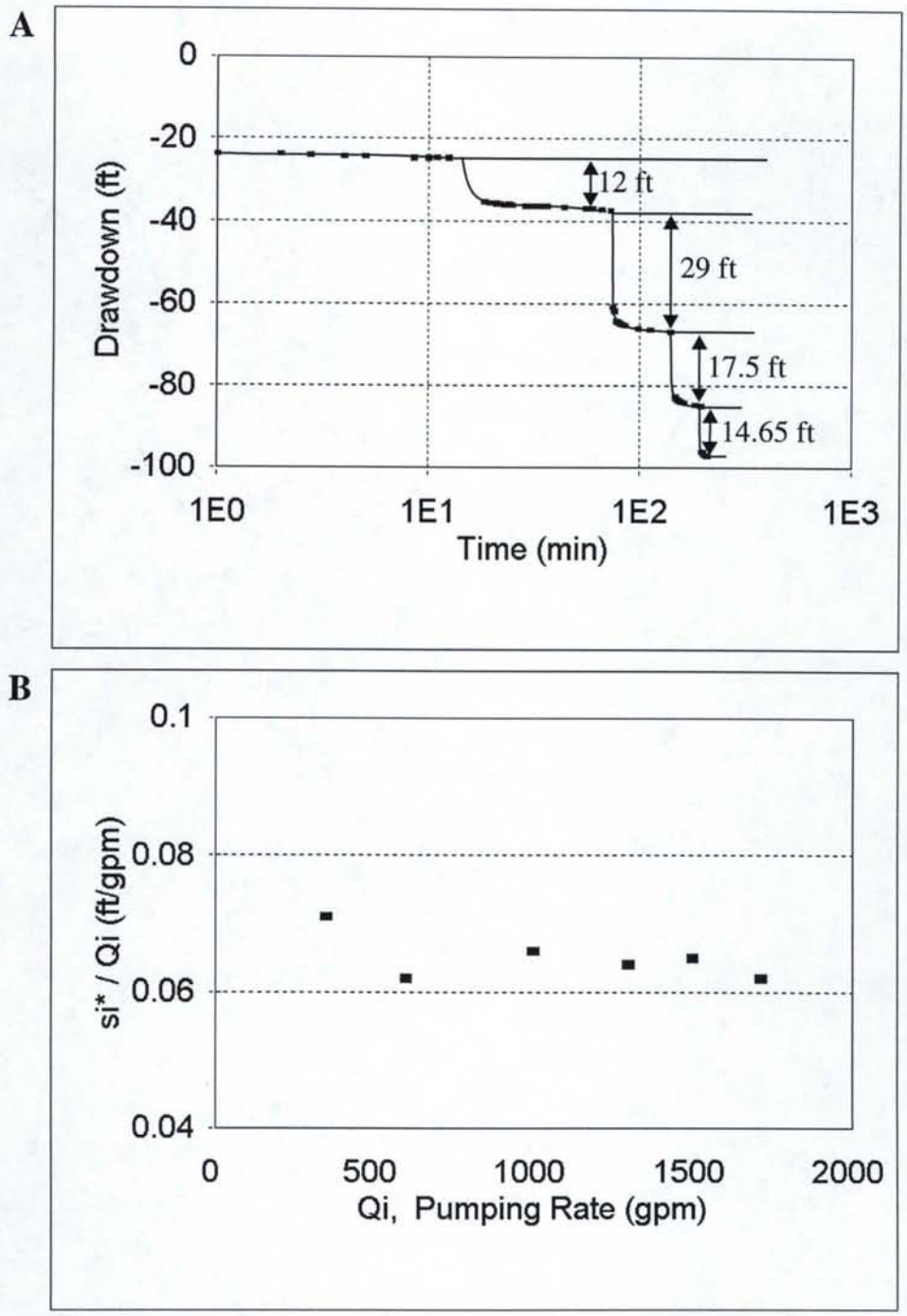

Figure 12. A. Semilog plot of drawdown vs time for step drawdown test. Incremental drawdown amounts are taken at the same elapsed time interval (50±1.5 min) for each step. Pumping rate, time and drawdown data for this plot are given in Table 1. B. Step drawdown data, including projected additional "step" from the constant-rate pumping test, plotted as drawdown (si*) per discharge rate (Qi) vs discharge rate (see Hantush, 1964) show constant rather than increasing trend indicating minimal non-linear well loss.

Non-leaky, infinite aquifer model

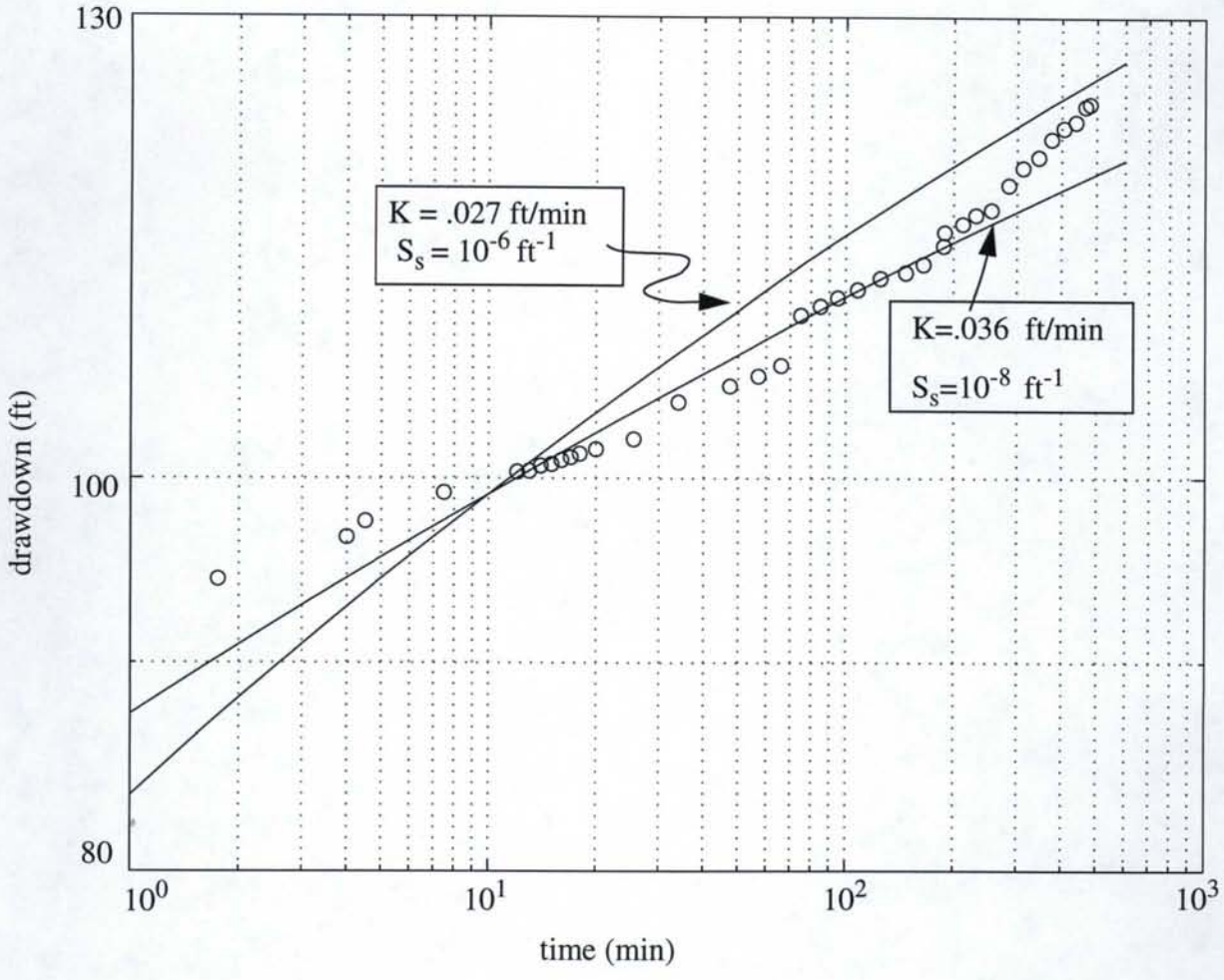

Figure 13. Log-log plot of drawdown vs time using Theis conceptual model and attempting to match pre-boundary measurements at the Goddard2 well during the constant-rate pumping test. Using T=3.6 ft^2/min (K=.036 ft/min) from semilog straight-line analysis by Mills (1991) requires an S_s value of 10^{-8} ft^{-1} for a fit to most of the measured data. Using a more reasonable S_s value of 10^{-6} ft^{-1}, T must be adjusted to 2.7 ft^2/min (K=.027 ft/min) to get a best fit with measured data - but this fit is worse than that for T=3.6 ft^2/min, and is poor overall.

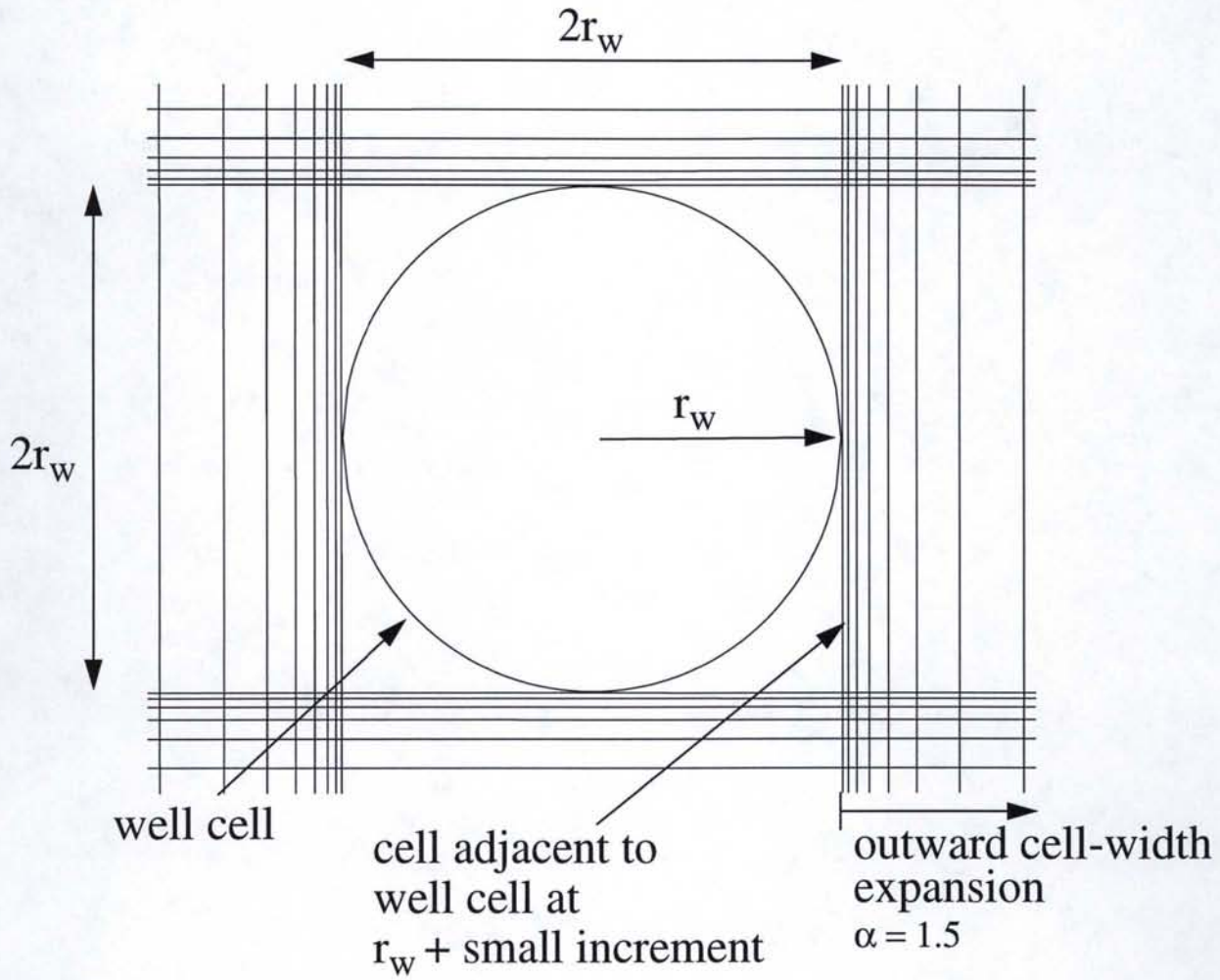

Figure 14. Discretization scheme in MODFLOW: width of well cell is well diameter; width of cell adjacent to well cell (at well-radius distance from center of well cell) is given a small width relative to the well cell. Cell widths outward from this small-width cell increase progressively by a factor of $\alpha = 1.5$.

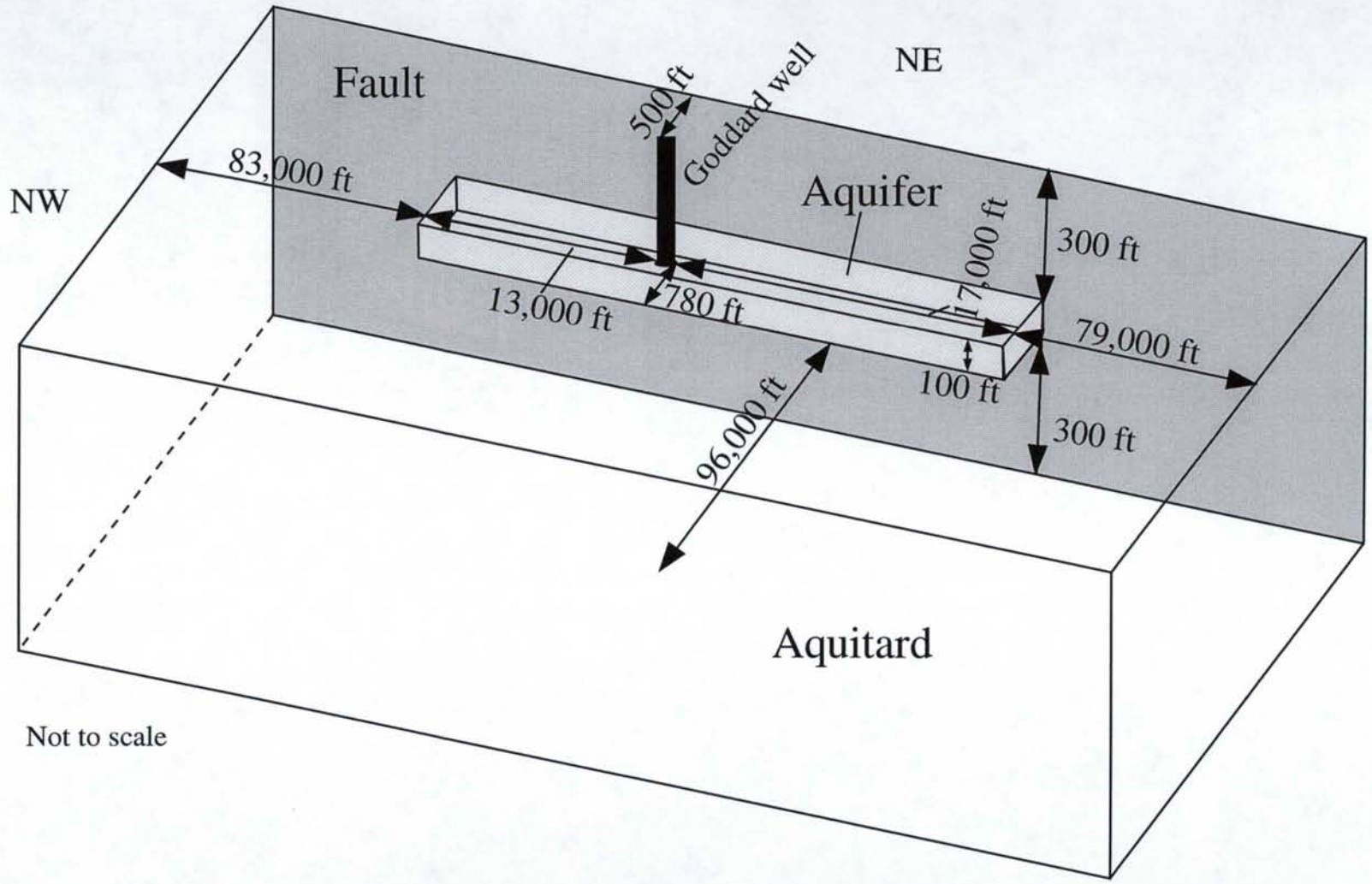

Figure 15. Schematic diagram of hydrologic system modeled for Goddard2 well pumping test. Aquifer is modeled as a sand stringer surrounded by fine–grained sediments and an impermeable boundary (fault) truncating the stringer on the northeast side. Outer boundaries are no–flow boundaries. Not to scale.

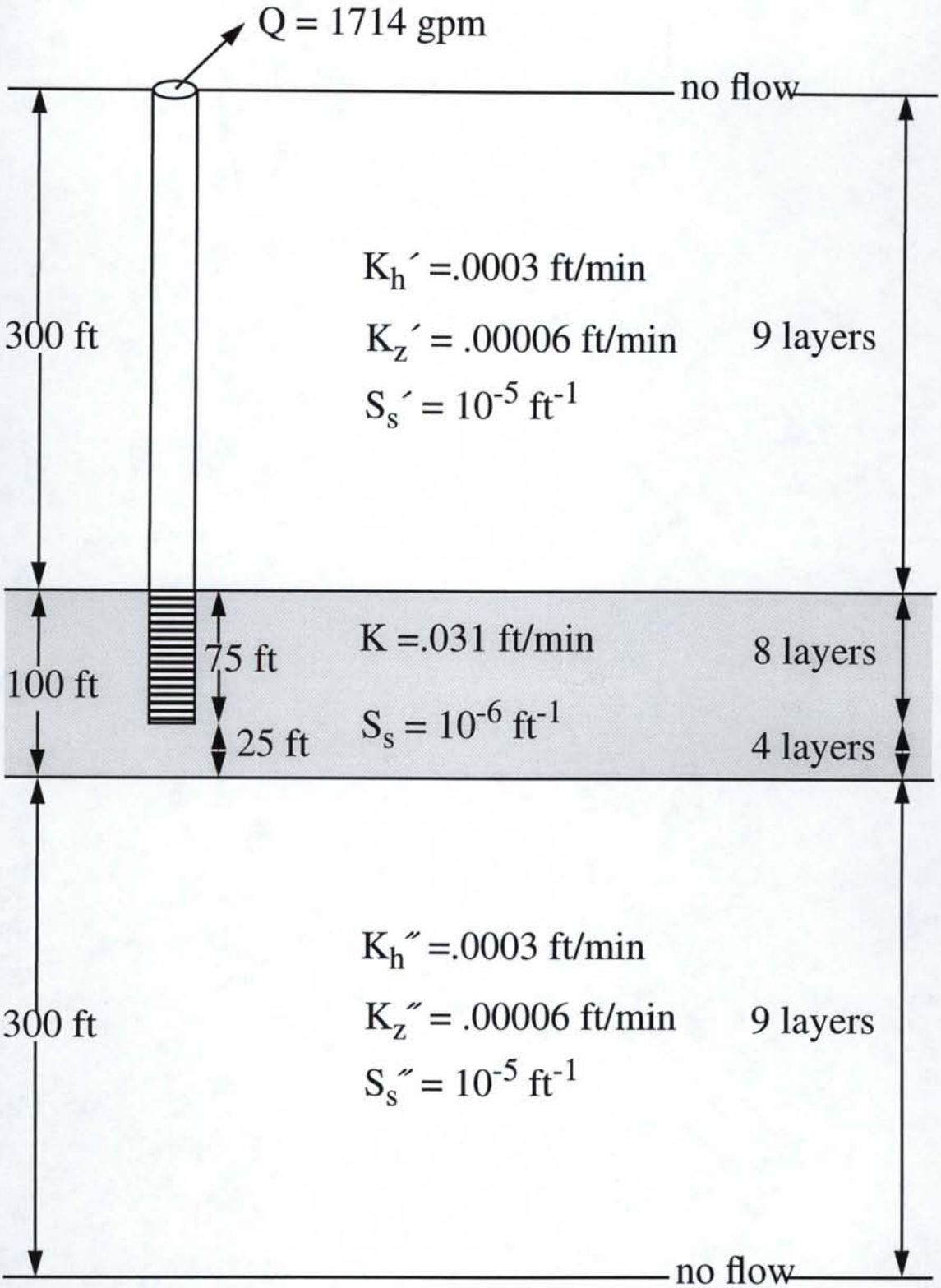

Figure 16. Section through hydrostratigraphic units and the partially penetrating pumping well showing dimensions, hydraulic parameters and discretization of model layers (see Table 5).

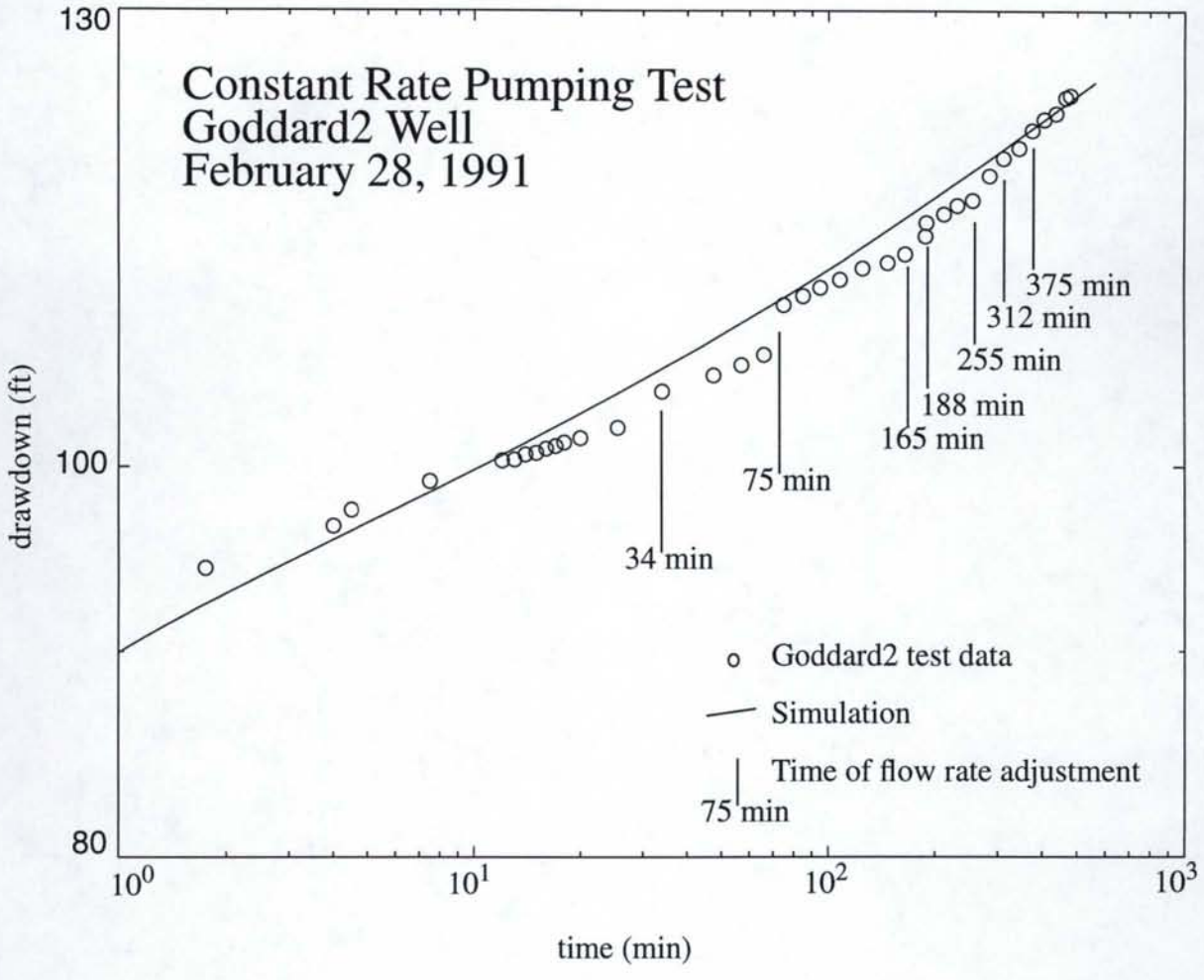

Figure 17. Log-log drawdown vs time plot for constant-rate pumping test at the Goddard2 well showing measured and simulated behavior. Note repeated pumping rate adjustments to counter downward drift (see Table 2).

APPENDIX A. MODELING AXIALLY SYMMETRIC AND NON-SYMMETRIC FLOW TO A WELL WITH MODFLOW

MODELING AXIALLY SYMMETRIC AND NON-SYMMETRIC FLOW TO A WELL WITH MODFLOW

INTRODUCTION

Tools for analyzing aquifer test data at the pumping or injection well (hereafter referenced as pumping well only) are limited for aquifer conditions that are not axially symmetric about the pumping well. Although the exact meaning of aquifer test interpretations from data at a pumping well may be complicated by well construction, well development and well efficiency issues, analysis of test data from pumping wells is necessary for single-well tests in non-ideal or complex hydrologic settings, and for multiple-well tests where observation wells do not respond. Analysis of data at the pumping well is valuable where few observation wells are available and where responses in observation wells are ambiguous, or where heterogeneity or multiple boundaries are known to be significant for the scale of the aquifer test.

Finite-difference models with rectilinear grid geometry such as MODFLOW (McDonald and Harbaugh, 1988) generally have not been used to simulate aquifer test results at a pumping well because they are not designed or expected to closely simulate head changes in pumping wells (e.g., Anderson and Woessner, 1992, p. 147). Head gradients in the vicinity of the pumping well are large and commonly are underestimated in conventional discretization schemes because distances between adjacent cell centers or nodes next to the well are too great to capture the steep and rapidly changing head gradients there.

This Appendix describes and demonstrates a discretization scheme which uses the rectilinear grid system of MODFLOW to accurately model well hydraulics in a variety of test-case scenarios. Although an axisymmetric, node-centered, adaptation of MODFLOW exists (Reilly and Harbaugh, 1993) which is many times more efficient than the scheme presented here for axisymmetric scenarios, we are not aware of another model that has accurately simulated transient responses at a well for non-axisymmetric flow or non-radially symmetric aquifer conditions. However, such flow and aquifer conditions are common in heterogeneous media and in environments with complex boundary and induced-stress configurations. And such a capability with MODFLOW might be extended further in conjunction with other modeling codes that accept MODFLOW results as input, such as contaminant or tracer transport modeling with MT3D (Zheng, 1992) and parameter estimation with MODFLOWP (Hill, 1992).

DISCRETIZATION SCHEME

The discretization scheme presented here uses twice the effective well radius as the X and Y (column and row) dimensions of the cell containing the pumping well (the "well cell"), and then moves outward from the well cell with increasing cell widths starting with a cell width that is a small fraction of the well diameter (Figure A1). By having very small cell widths near the well cell, errors associated with finite-differencing of distance between nodes are small. Also, intensity of discretization and symmetry of cell dimensions increase to a maximum at the corners of the well cell, and at outward projections of those corners throughout the grid.

In this geometry, cells with the poorest aspect ratios are located along and near streamlines at 90° intervals where their short dimensions and nodes are aligned or nearly aligned with the direction of flow to best capture steep gradients, and their long dimensions are more nearly "aligned" with head contours where head change along the long dimension (crossing streamlines) is small (Figure A2). Conversely, with approach to a corner along a row or column, cell dimensions become progressively more equal with the longer dimension decreasing in length as rate of head change increases in the respective column or row direction - until increases in head change relative to X and Y coordinates are nearly equal and maximum at corners where, also, cell dimensions are equal and minimum (Figure A2). With this geometry, effects of converging flow (e.g., curvature of head contours and steep, rapidly changing head gradients) can be simulated accurately near the pumping well.

Drawdown at the pumping well is represented by drawdown not in the actual well cell but at any of the four cells immediately surrounding the well cell that is at $r = r_w$ + very small increment (Figure A1). In this Appendix we assume that the head measured in the formation immediately outside the well (i.e., at $r = r_w$) is equal to the head in the well. This is a reasonable assumption in well hydraulics where well losses and/or well storage contributions to discharge may be neglected (Hantush, 1964; Papadopoulos and Cooper, 1967). This assumption is based on continuity considerations where the water level in the well equals the head at the well screen and the pumping rate from the well equals the flow rate into the well across the cylindrical surface at r_w.

Similarly, axisymmetric finite-difference (Reilly and Harbaugh, 1993) and finite-element (Akindunni et al, 1995; Akindunni and Gillham, 1992) numerical models designed specifically to simulate aquifer behavior in response to well stresses have their axes of symmetry at the well center (outside the actual model domain) but have their initial column of nodes located at r_w, at the edge of the actual model domain. In MODFLOW, pumpage is independent of head and is assigned at the well cell node (McDonald and Harbaugh, 1988), which is analagous to pumpage from a line sink as in classic analytical solutions (e.g., Theis, 1935; Hantush, 1960) - so, in the discretization scheme presented here, the head or drawdown values in the well cell are some intermediary value between those at r_o in an aquifer pumped from a line sink well with no radial length and those at r_w (cell adjacent to the well cell). That is, well cell head or drawdown values do not correspond to a measurable or theoretical feature in a well-aquifer system.

The cell-width expansion factor used here, α, is the same as that used by Reilly and Harbaugh (1993) for their axisymmetric adaptation of MODFLOW:

$$\alpha = r_{i+1} / r_i$$

where r is the radial distance to a node, i is the index number of the "column" or radial shell outward from the well, and α is generally given a value between 1.2 and 1.5. In this Appendix, grids for simulations with the MODFLOW discretization scheme described here all use $\alpha = 1.5$ but have different relative widths for the first cell adjacent to the well cell, with widths relative to the well cell ranging from .002 to .03 (Table A1). For layered systems or systems with partially penetrating wells, discretization of layer thicknesses should be approached as in other modeling problems: find

the scheme that adequately captures the essential system behavior for the problem under investigation with the minimum of set-up and computing cost.

BENCHMARKING

The MODFLOW discretization scheme presented here is benchmarked against analytical solutions and RADMOD, the axially symmetric application of MODFLOW (Reilly and Harbaugh, 1993), for three axially symmetric scenarios, and against the analytical solution for one non-axisymmetric scenario (multiple no-flow boundaries). Model parameters are given in Table A1 for the different scenarios and models run. All MODFLOW and RADMOD runs used the SIP solver with the same input specifications (Table A2). Analytical and RADMOD models were run on a PC with a 486 processor; MODFLOW models were run on a DEC Alpha workstation.

The model domain is 1/4 of the full domain for the axially symmetric scenarios to minimize model set-up and computation time. Pumping well dimensions and pumping rates are reduced (well cell diameter is 0.5 full diameter; pumping rate is 0.25 full pumping rate) to account for this scaling. This approach is valid in media with all hydrogeologic units having horizontally isotropic permeability (i.e., principal permeability directions parallel to the X and Y grid axes), because no flow will occur across the X and Y axes under radial flow conditions. That is, in a system with axially symmetric flow to a well, streamlines are coincident with grid lines at 90° intervals in a rectilinear grid representing that system and, by definition, no flow occurs across streamlines (e.g., Anderson and Woessner, 1992).

In this Appendix, drawdown behavior is compared at the pumping well - where numerical model capabilities for simulating radially converging flow with steep and rapidly changing gradients are most severely tested for a rectilinear grid. It should be noted that, for all scenarios, drawdown behavior was examined at nearby observation wells (r_{obs} in the range of 20 to 30 ft) located at off-diagonal and off-axis positions (i.e., row index not equal to column index, and row index and column index not equal to 1). Results are essentially identical at observation wells with analytical and numerical models for all four scenarios, and so are shown here as an example only for one scenario, the non-symmetrical multiple-boundary scenario (Scenario 4).

SCENARIO 1. NON-LEAKY AQUIFER

The analytical solution for drawdown at a given radius and time due to pumping from a line sink in a confined, non-leaky aquifer of infinite areal extent was given by Theis (1935). The particular conditions modeled in scenario 1 are shown in Figure A3. The analytical solution was generated using the code of Moench and Ogata (1984). Model performances at the well (r_w) as log-log time-drawdown curves are given in Figure A4. MODFLOW results using the discretization scheme described above (and $\alpha = 1.5$) compare well with analytical or RADMOD solutions, especially at times likely to be measurable in a real aquifer test. However, MODFLOW results using a discretization scheme with outward cell-width expansion from the well cell (not from a small-width cell adjacent to the well cell) remains below the analytical solution for the full duration of the 1000 min test, even with α set at 1.3 (Figure A4).

SCENARIO 2. AQUIFER RECEIVING LEAKAGE FROM STORAGE IN AQUITARD

Hantush (1960) gave the analytical solution for drawdown at a given radius and time in a confined aquifer due to pumping from a line sink in the aquifer which is receiving leakage from storage in an aquitard that is bounded by a no-flow boundary. The particular conditions modeled in scenario 2 are shown in Figure A5. The analytical solution was generated using the code of Moench and Ogata (1984).

The two hydrostratigraphic units (aquitard and aquifer) in this scenario are discretized into a number of model layers each in RADMOD and MODFLOW models (Table A1) to account for the fact that head distribution is not uniform vertically in these hydrostratigraphic units. Vertical discretization is progressively finer approaching the interface between the aquifer and aquitard. Pumping was distributed proportionally between the well cells in the aquifer model layers on the basis of percent thickness of a given aquifer layer (symbols are defined in Notation section below):

$$Q = \sum Q_i \ ; \ \text{where } Q_i = Q * (b_i/b)$$

Similarly, drawdown in the pumping well was determined as the weighted average of drawdowns in a column of aquifer cells at r_w based on percent thickness of a given aquifer layer compared to the aquifer as a whole:

$$\Delta s = \sum \Delta s_i \ ; \quad \text{where } \Delta s_i = \Delta s * (b_i/b)$$

Model performances are shown in Figure A6. MODFLOW results compare well with analytical or RADMOD solutions, especially at times likely to be measurable in a real aquifer test. It should be noted that better early-time matches with MODFLOW (for this and other scenarios) can be achieved by discretizing the first period more intensely or adding an earlier period, but the practical benefit for the additional computation time may be minimal because field data rarely are available for elapsed times much less than .02 min.

SCENARIO 3. PARTIALLY PENETRATING WELL PUMPING FROM AN AQUIFER WITH RADIAL-TO-VERTICAL ANISOTROPY OF PERMEABILITY

Neuman (1974) gave the analytical solution for drawdown at a given radius, time and measuring point or depth interval in an unconfined aquifer pumped with a partially penetrating well. This solution also included permeability anisotropy between radial and vertical permeabilities. To avoid problems with large drawdowns relative to aquifer thickness above the pumping well for an unconfined system, this scenario was modeled for a confined system (particular conditions are shown in Figure A7). The analytical solution was generated using the code of Moench (1993).

Vertical discretization was intensified in layers above and below the top of the partially penetrating well to capture steep vertical gradients there. Apportionment of pumping and drawdown were made in a manner similar to that described for scenario 2, except that the normalizing thickness used to apportion pumpage and to weight drawdown contributions was the screen thickness, not the aquifer thickness. Model performances are given in Figure A8. MODFLOW results compare well with

analytical or RADMOD solutions after the initial few minutes of the aquifer test.

SCENARIO 4. AQUIFER WITH INTERSECTING NO-FLOW BOUNDARIES

Drawdown at wells in a confined non-leaky aquifer influenced by no-flow boundaries of favorable geometry (e.g., linear boundaries with right-angle intersections) may be expressed analytically as the superposition of drawdowns due to a set of three image wells that produce the effects of the boundaries relative to the real pumping well (same as example of Domenico and Schwartz, 1990, p. 180). This scenario is not axially symmetric and so the MODFLOW discretization scheme is benchmarked only against the analytical solution. The aquifer extent, wells (real and image wells), and boundary conditions for scenario 4 are shown in Figure A9A for the pumping well, and in Figure A9B for an observation well. Model performances are given in Figures A10A and A10B. Again, MODFLOW results using the discretization scheme described here compare well with the analytical solution, especially at times likely to be measurable in a real aquifer test.

SUMMARY

Drawdown at a well can be modeled accurately in MODFLOW with a discretization scheme where the X and Y (column and row) dimensions of the cell containing the well are equal to the effective diameter of the well, where the cells adjacent to the well cell along orthogonal grid-axis directions have very small cell widths, and where cell widths increase progressively outward with an expansion factor, α, of 1.2 to 1.5. The validity of this discretization scheme has been demonstrated for simulation of drawdown responses at a pumping well in a confined aquifer in four scenarios, three axisymmetric and one non-symmetric. More efficient solutions to axisymmetric systems modeled here exist, but tools for analysis of drawdown at or near the pumping well in complex layered systems and systems with multiple boundaries are otherwise not available. By logical extension, MODFLOW can be used to simulate drawdown accurately at a well in a heterogeneous aquifer because MODFLOW can model three-dimensional flow in a heterogeneous aquifer system and the limitations on accuracy of drawdown simulations at a well are related to discretization near the well and are not inherent in the model structure.

NOTATION

b	aquifer thickness, L
b_i	thickness of layer i in the aquifer, L
b'	aquitard thickness, L
K	aquifer hydraulic conductivity, LT^{-1}
K'	aquitard hydraulic conductivity, LT^{-1}
K_r	aquifer radial hydraulic conductivity, LT^{-1}
K_r'	aquitard radial hydraulic conductivity, LT^{-1}
K_z	aquifer vertical hydraulic conductivity, LT^{-1}
K_z'	aquitard vertical hydraulic conductivity, LT^{-1}
Q	pumping rate, L^3T^{-1}
Q_i	pumping rate in layer i, L^3T^{-1}
r	radius or distance, L
r_o	center of well, L

r_w well radius, L
r_{il} distance to a given (subscript number) image well, L
S_s aquifer specific storage, L^{-1}
S_s' aquitard specific storage, L^{-1}
s drawdown, L
s_i drawdown in layer i, L
α grid expansion rate factor

REFERENCES CITED

Akindunni, F. F. and Gillham, R.W., 1992, Unsaturated and saturated flow in response to pumping of an unconfined aquifer: Numerical investigation of delayed drainage: Ground Water, v. 30, no. 6, p. 873-884.

Akindunni, F.F., Gillham, R.W., Conant, B., Jr., and Franz, T., 1995, Modeling of contaminant movement near pumping wells: Saturated-unsaturated flow with particle tracking: Ground Water, v. 33, no. 2. p. 264-274.

Anderson, M.P. and Woessner, W.W., 1992, Applied Ground Water Modeling: Academic Press, Inc., New York, 381 p.

Domenico, P. A. and Schwartz, F.W., 1990, Physical and Chemical Hydrogeology: John Wiley & Sons, New York, 824 p.

Hantush, M. S., 1960, Modification of the theory of leaky aquifers: Journal of Geophysical Research, v. 65, no. 11, p. 3713-3725.

Hantush, M. S., 1964, Hydraulics of wells, in V.T. Chow, ed., Advances in Hydroscience, 1, Academic Press, New York.

Hill, M.C., 1992, A computer program (MODFLOWP) for estimating parameters of a transient, three-dimensional, ground-water flow model using nonlinear regression: U.S. Geological Survey Open-File Report 91-484, 358 p.

McDonald, M.G. and Harbaugh, A.W., 1988, A modular three-dimensional finite-difference ground water flow model: U.S. Geological Survey Techniques of Water-Resources Investigations Book 6, Chapter A1.

Moench, A.F., 1993, Computation of type curves for flow to partially penetrating wells in water-table aquifers: Ground Water, v. 31, no. 6, p. 966-971.

Moench, A.F. and Ogata, A., 1984, Analysis of constant discharge wells by numerical inversion of Laplace transform solutions, in Rosenshein, J.S., and Bennett, G.D., eds., Groundwater Hydraulics, American Geophysical Union Water Resources Monograph 9, p. 146-170.

Neuman, S.P., 1974, Effect of partial penetration on flow in unconfined aquifers considering delayed gravity response: Water Resources Research, v. 10, no. 2, p. 303-312.

Papadopoulos, I.S. and Cooper, H.H., Jr., 1967, Drawdown in a well of large diameter: Water Resources Research, v. 3, no. 1, p. 241-244.

Reilly, T.E. and Harbaugh, A.W., 1993, Simulation of cylindrical flow to a well using the U.S. Geological Survey Modular Finite-Difference Ground-Water Flow Model: Ground Water, v. 31, no. 3, p. 489-494.

Theis, C.V., 1935, The relation between the lowering of the piezometric surface and the rate and duration of discharge of a well using groundwater storage: Transactions of the American Geophysical Union v. 16, p. 519-524.

Zheng, C., 1992, MT3D, A modular three-dimensional transport model for simulation of advection, dispersion and chemical reactions of contaminants in groundwater systems: S.S. Papadopoulos & Associates, Inc., Bethesda, MD.

Table A1. Numerical Model Characteristics

Model Scenario	Discretization Scheme	Rows (1)	Columns (2)	Layers (3)	Stress Periods	Time Steps (4)	r well cell	width of cell adj to well
1. No leakage (Theis, 1935)	MODFLOW (5)	40	40	1	4	85	.333 ft	.01 ft
	RADMOD	1	50	1	3	60	.333 ft	.107 ft
2. Leakage from storage in aquitard (Hantush, 1960)	MODFLOW (5)	35	35	24	4	100	0.5 ft	.01 ft
	RADMOD	12	60	1	4	100	0.5 ft	.15 ft
3. Partially penetrating well, anisotropic permeability (Kr>Kz)	MODFLOW (5)	45	45	25	4	80	.936 ft	.001667 ft
	RADMOD	26	60	1	2	70	.936 ft	.2808 ft
4. Intersecting no-flow boundaries	MODFLOW	100	100	1	3	90	.5 ft	.005 ft

(1) In RADMOD, rows are model layers
(2) In RADMOD, columns are radial shells
(3) In RADMOD, layer is a model feature that does not represent scenario geometry
(4) TSMULT, the multiplier for successive time steps in a given stress period is 1.2 for all runs
(5) Model domains are 1/4 of full domain; cell-width expansion factor is increased from 1.5 to 2 in outer regions of the model where gradients are low

Table A2. SIP input values for all MODFLOW and RADMOD runs.

Parameter Name	Parameter	Parameter Value
MXITER	Maximum iterations per time step	1000
NPARM	Number of iteration parameters	5
ACCL	Acceleration parameter	1
HCLOSE	Head-change conversion tolerance	.00001 ft
IPCALC	Flag (seed is given by user)	0
WSEED	Iteration parameter seed	.001

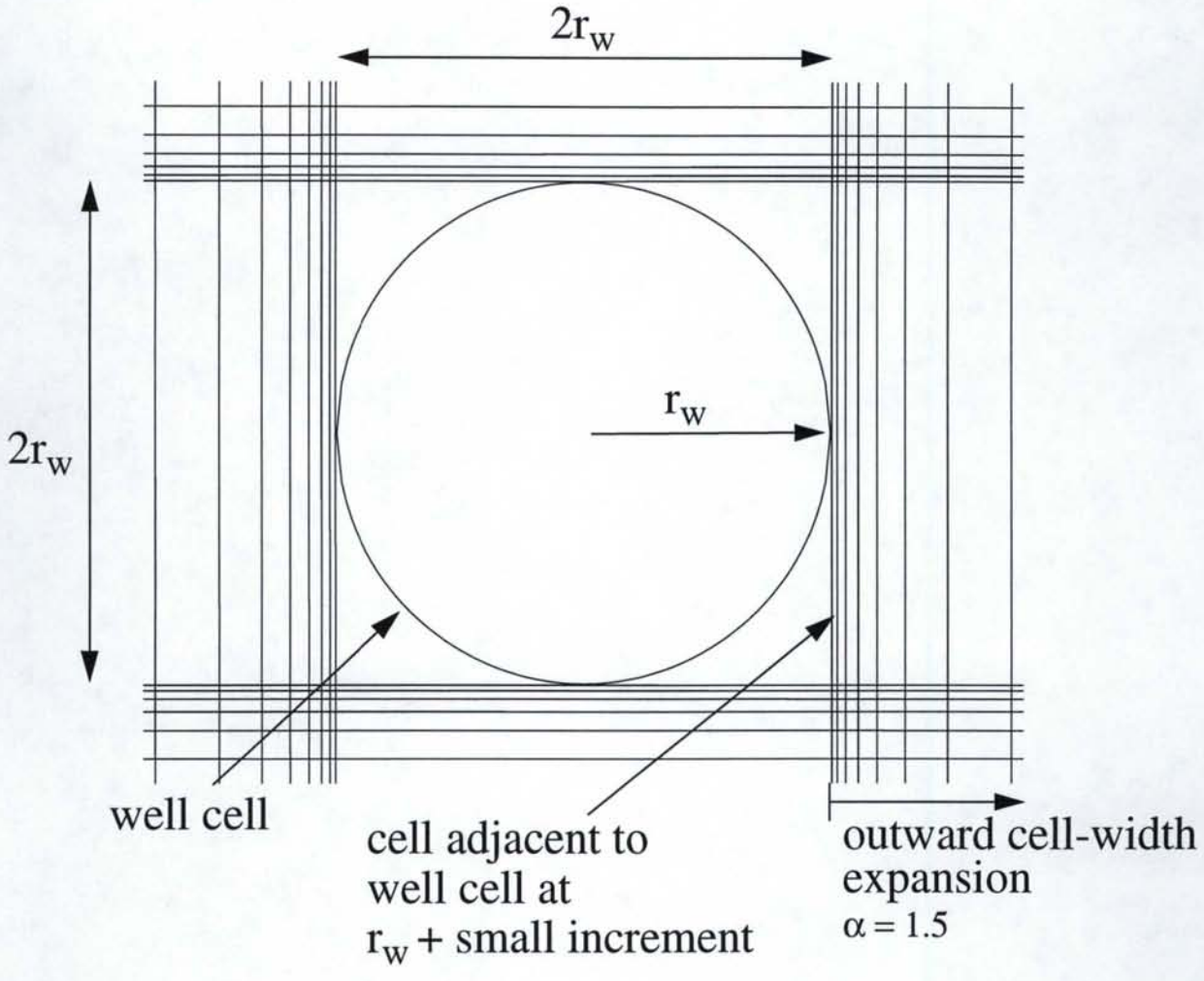

Figure A1. Discretization scheme: Width of well cell is well diameter. Width of cell adjacent to well cell (at well-radius distance from the center of the well cell) is given a small width relative to the well cell. Cell widths outward from this small-width cell increase progressively by a factor of $\alpha = 1.5$.

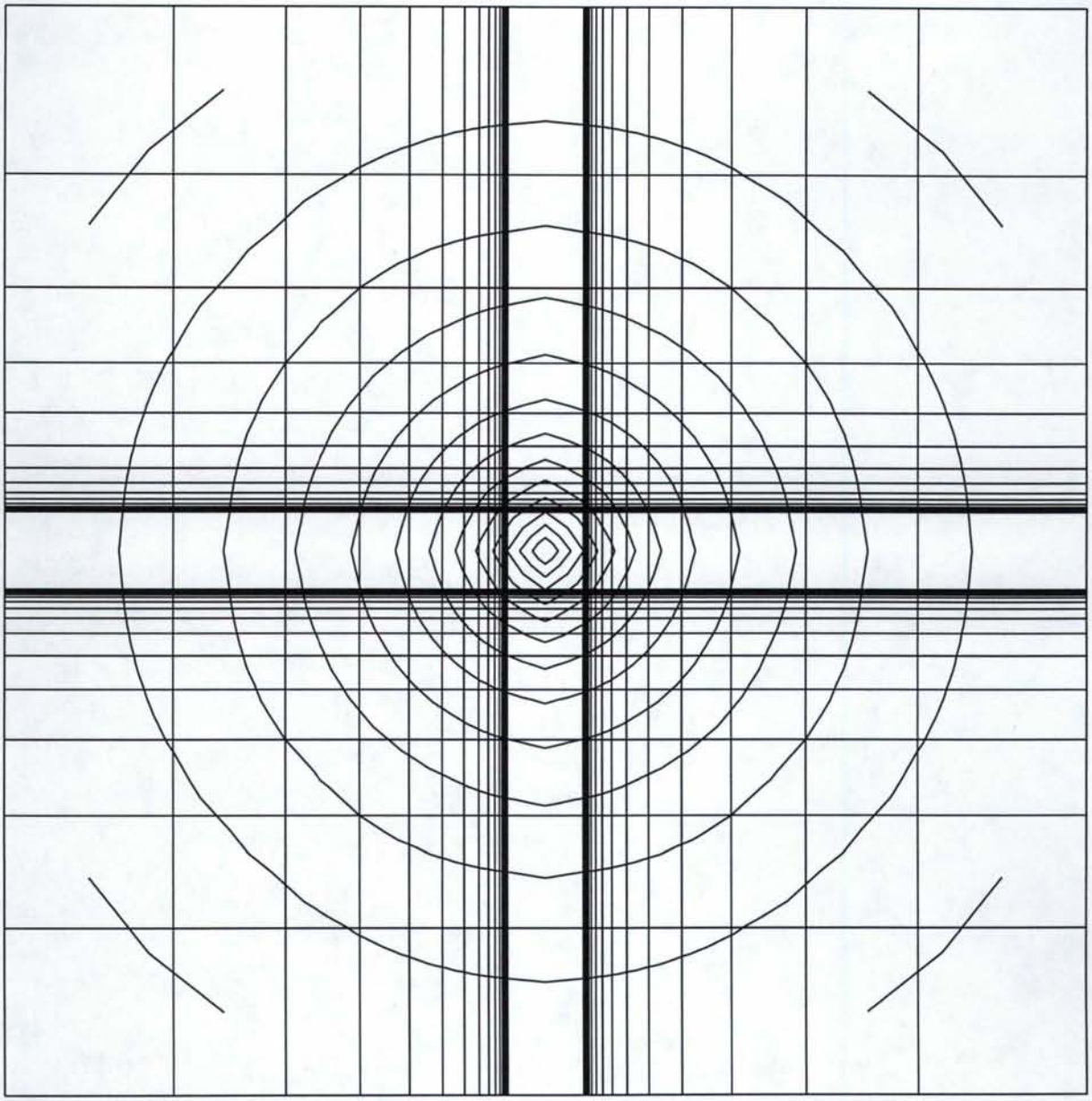

Figure A2. Well geometry, grid geometry and drawdown at the well. Drawdown at the well is accurately simulated by the finite-difference model because the grid discretization scheme locates nodes at the edge of the well and has dense discretization both outward from the well cell and around the curvature of the well cell corner.

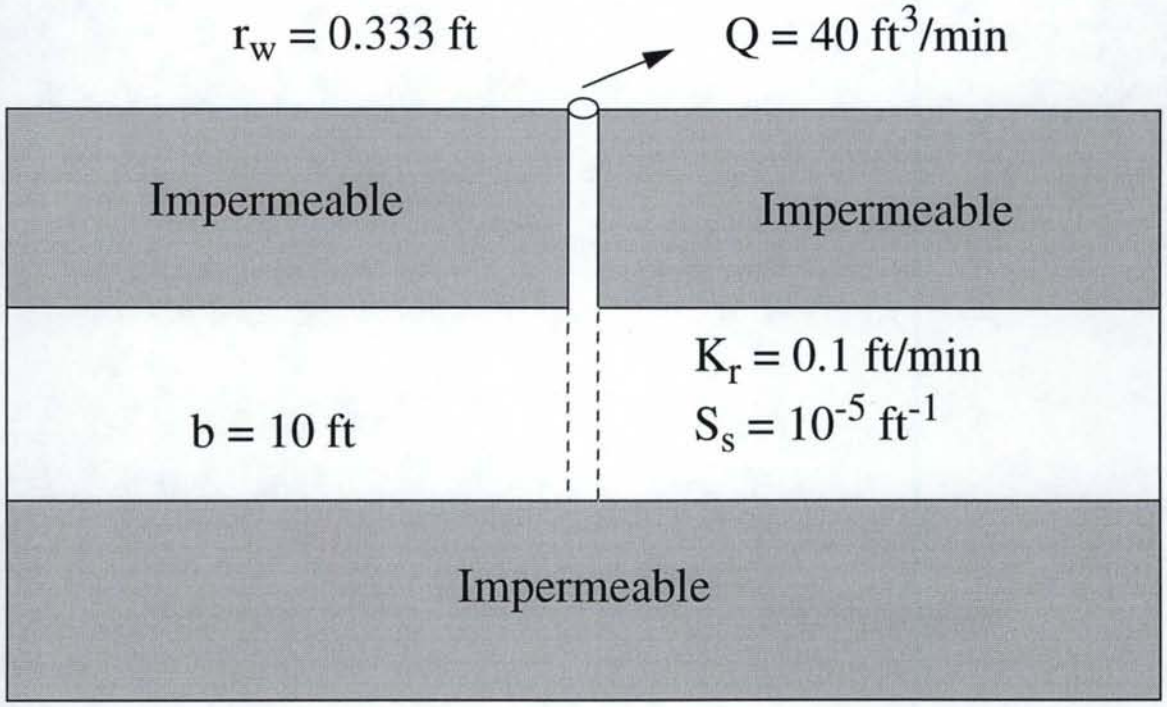

Figure A3. Scenario 1 - Theis conditions: Confined aquifer of infinite areal extent with no leakage.

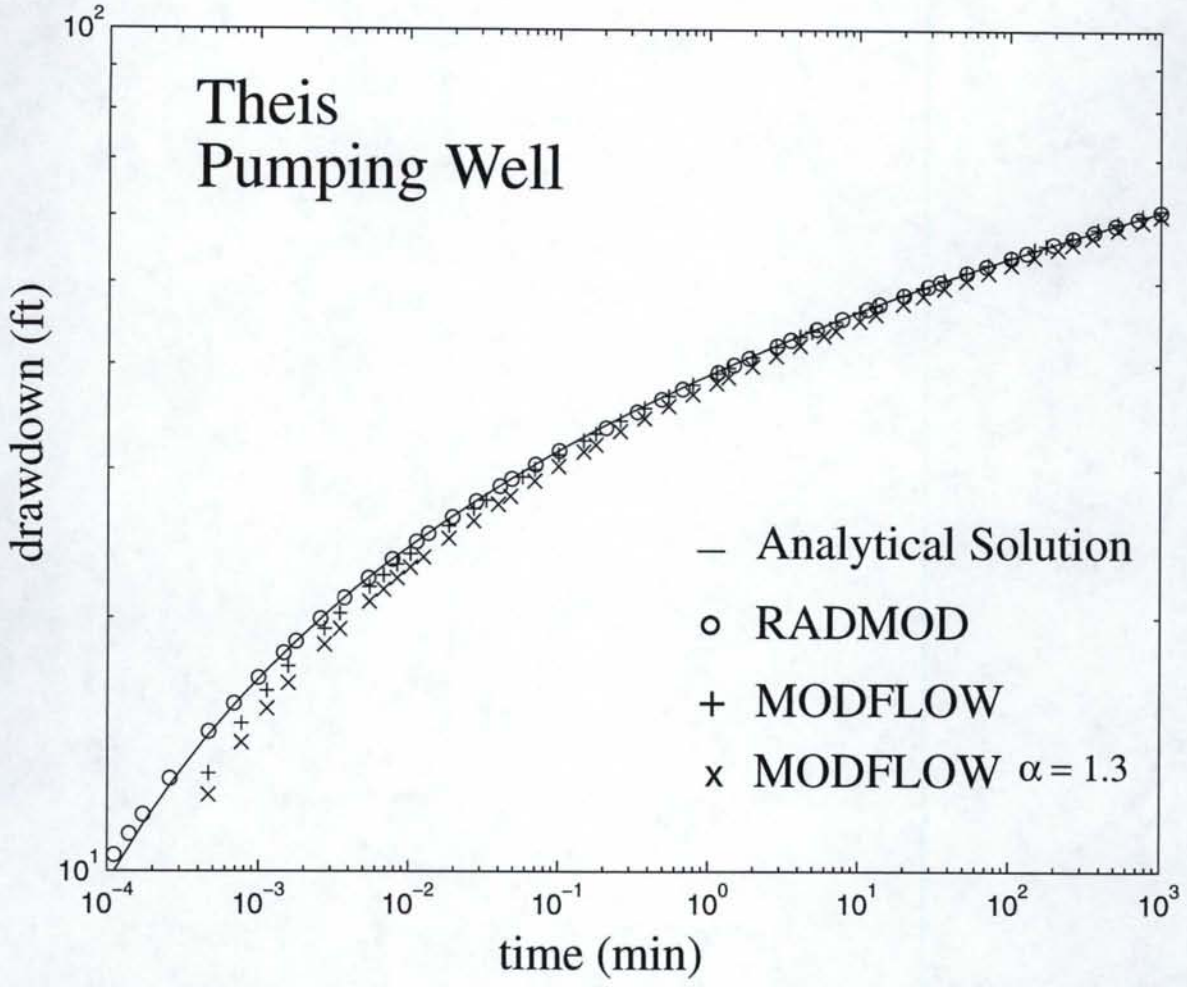

Figure A4. Comparison of model results at the pumping well for Scenario 1 - Theis conditions. MODFLOW reults with + symbol are generated with discretization scheme where cells adjacent to the well cell have a small width and cell widths expand outward with $\alpha = 1.5$. MODFLOW results with x symbol are generated with discretization scheme where cell widths expand outward from the well cell with $\alpha = 1.3$.

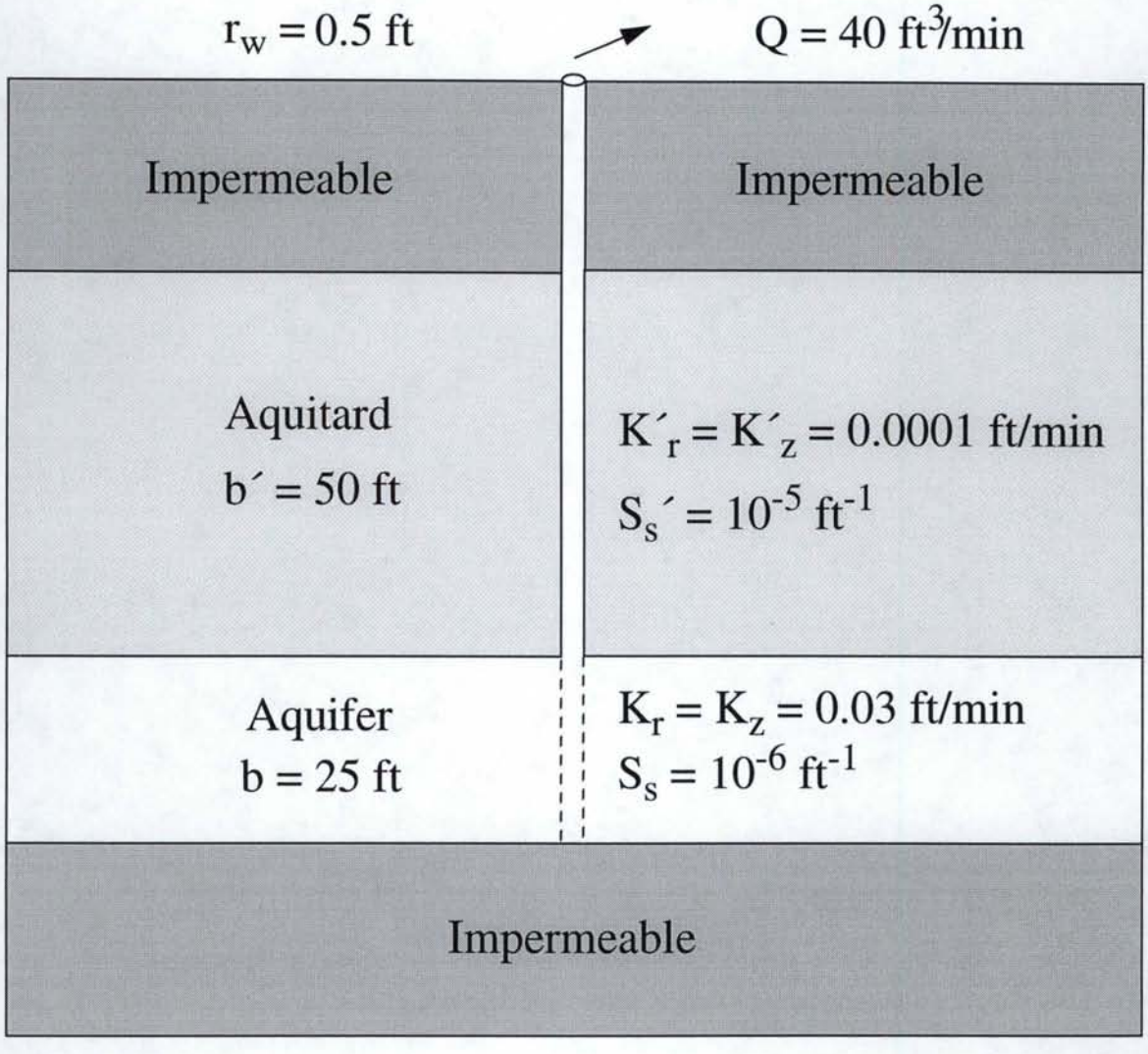

Figure A5. Scenario 2 - Hantush Case 2 conditions: Confined aquifer receiving leakage from an aquitard bounded by a no-flow boundary.

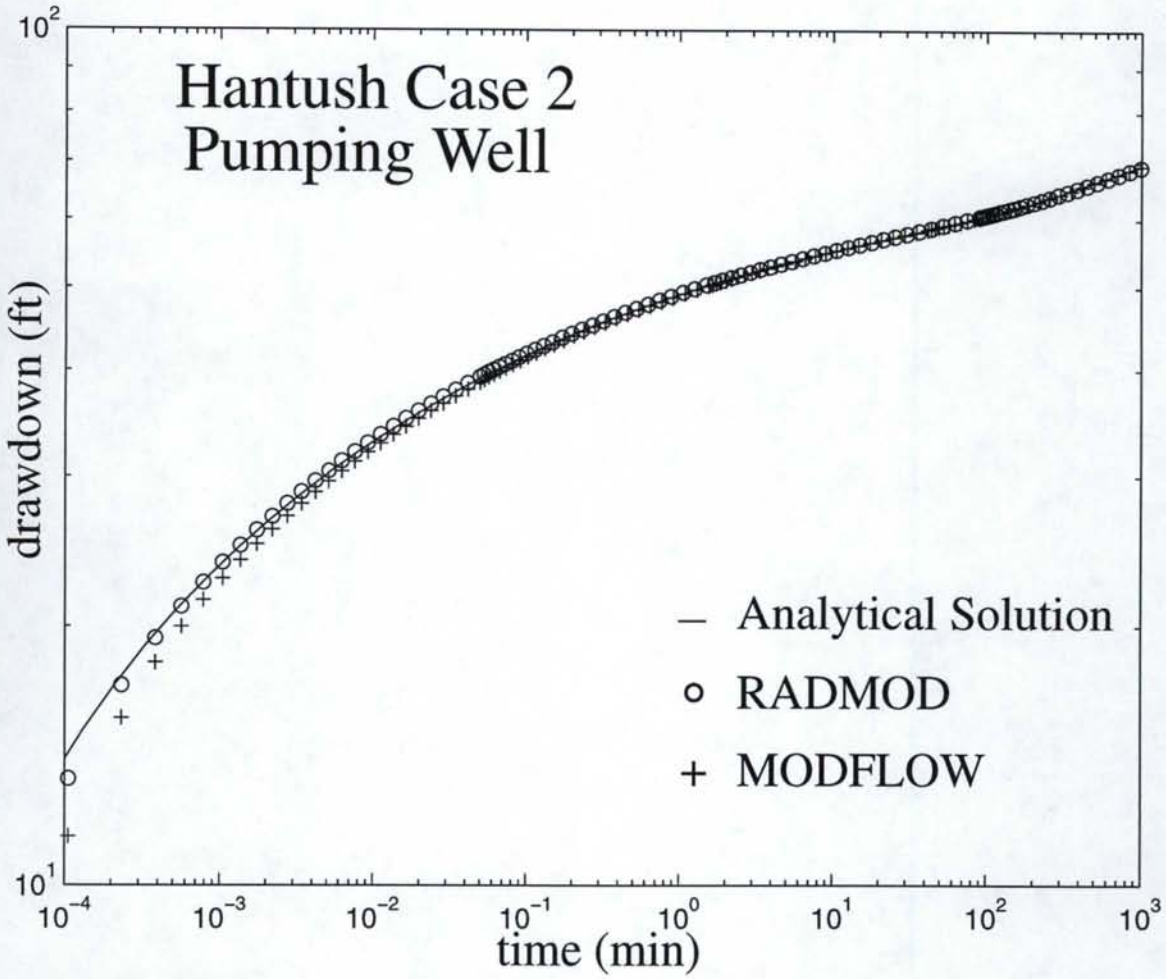

Figure A6. Comparison of model results at the pumping well for Scenario 2 - Hantush Case 2 conditions.

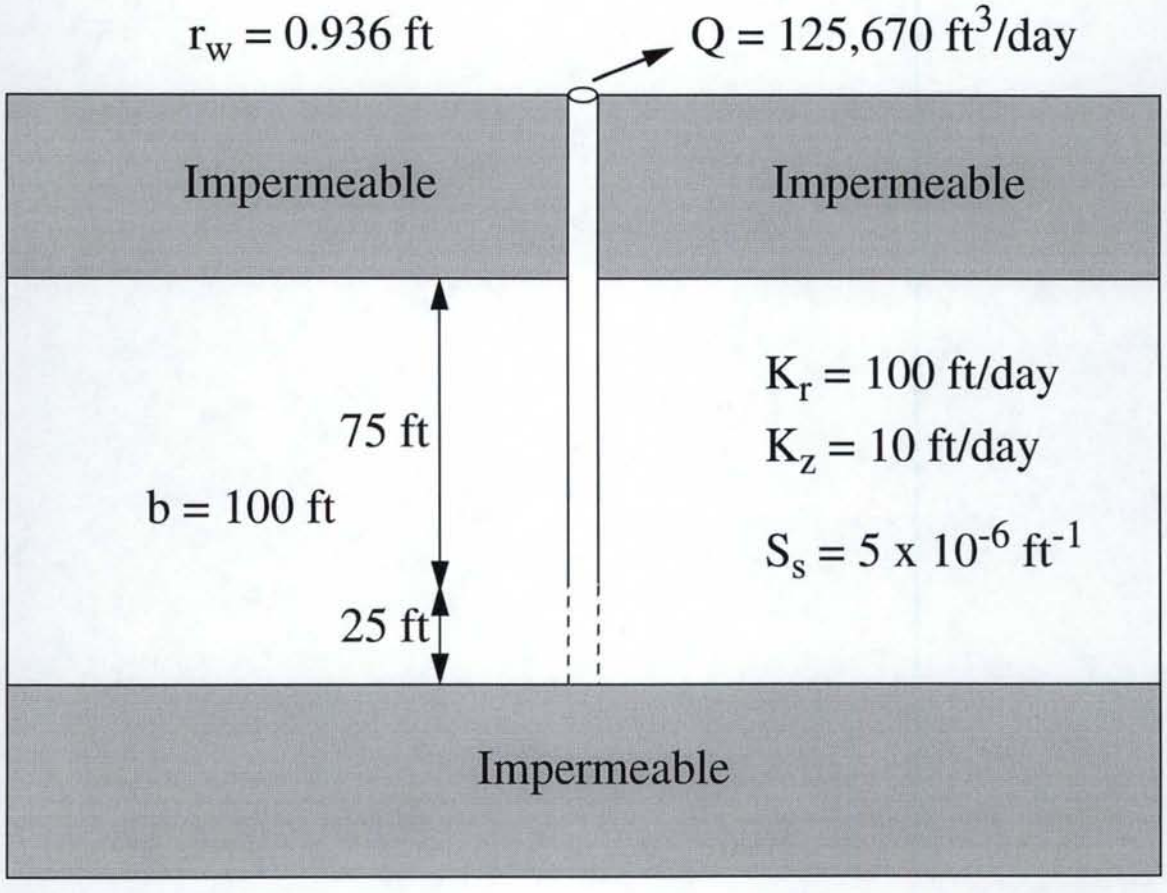

Figure A7. Scenario 3 - Partially penetrating pumping well in a confined, anisotropic aquifer.

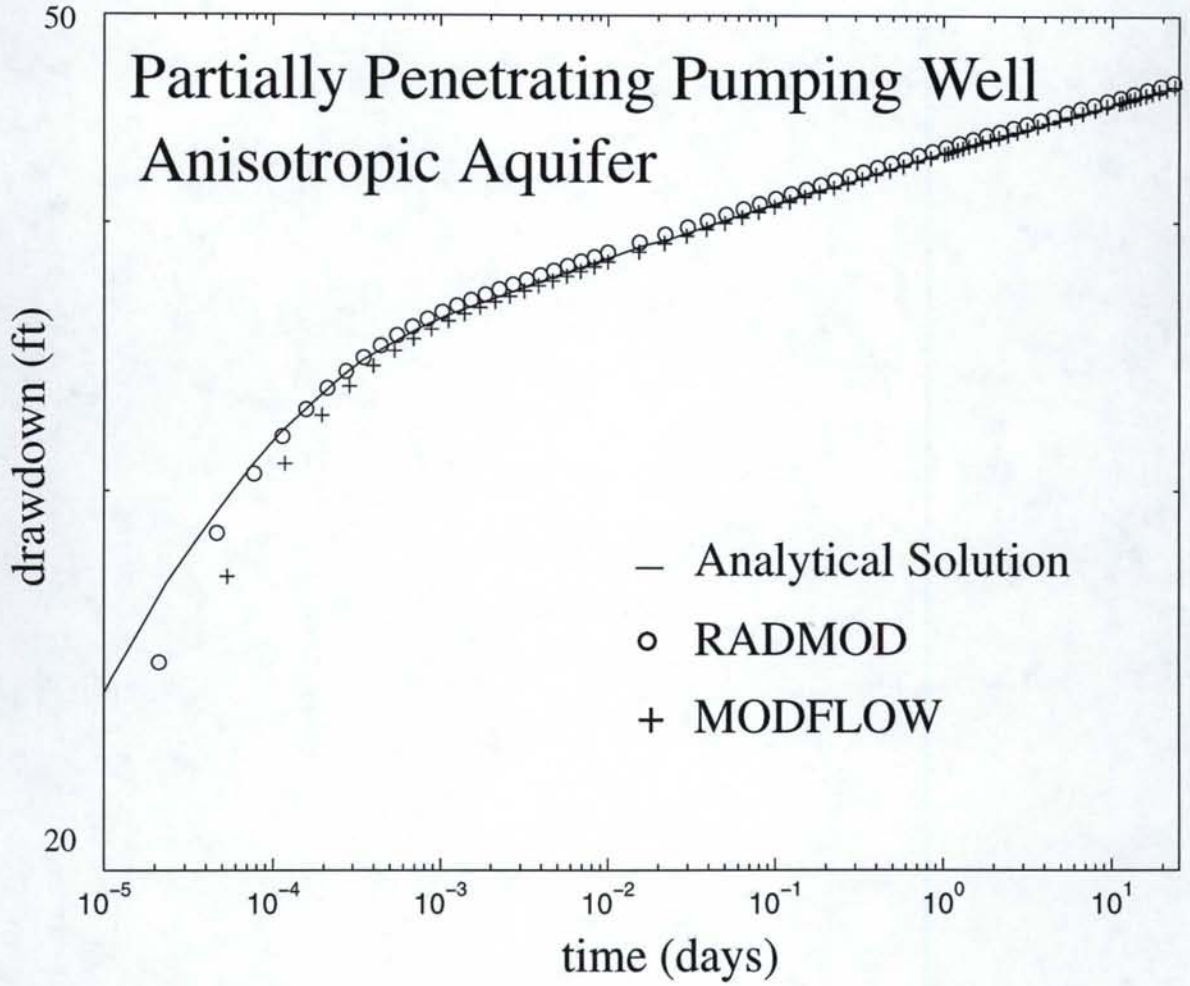

Figure A8. Comparison of model results at the pumping well for Scenario 3 - partially penetrating pumping well in a confined anisotropic aquifer.

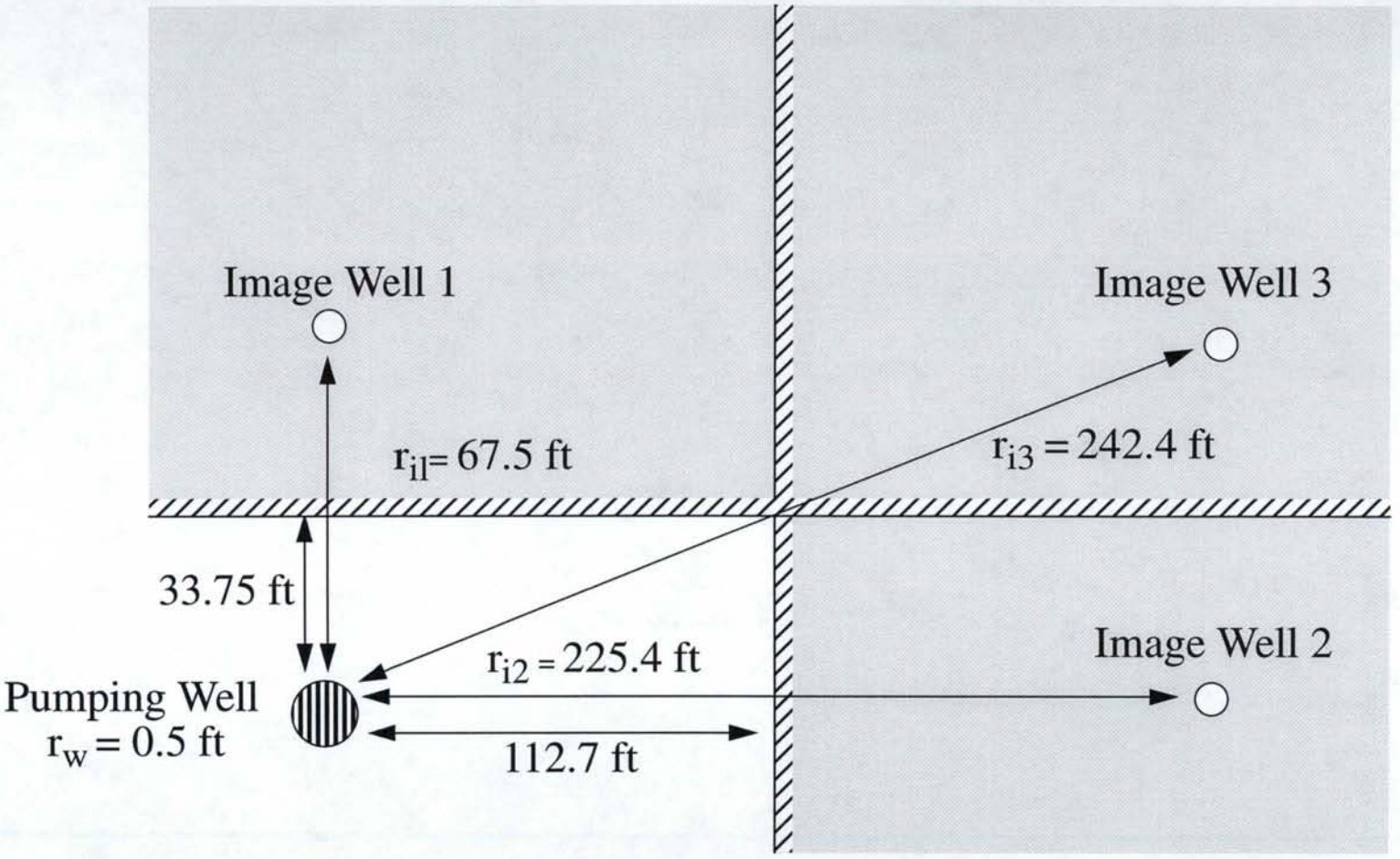

Figure A9A. Scenario 4 - Intersecting no-flow boundaries. For this scenario, Q = 30 ft^3 min^{-1}, b = 25 ft, K = .1 ft min^{-1}, and S_s = .0001 ft^{-1}. Relative positions of wells (real pumping well and image wells) and no-flow boundaries shown here were used in model with results shown in Figure A10A.

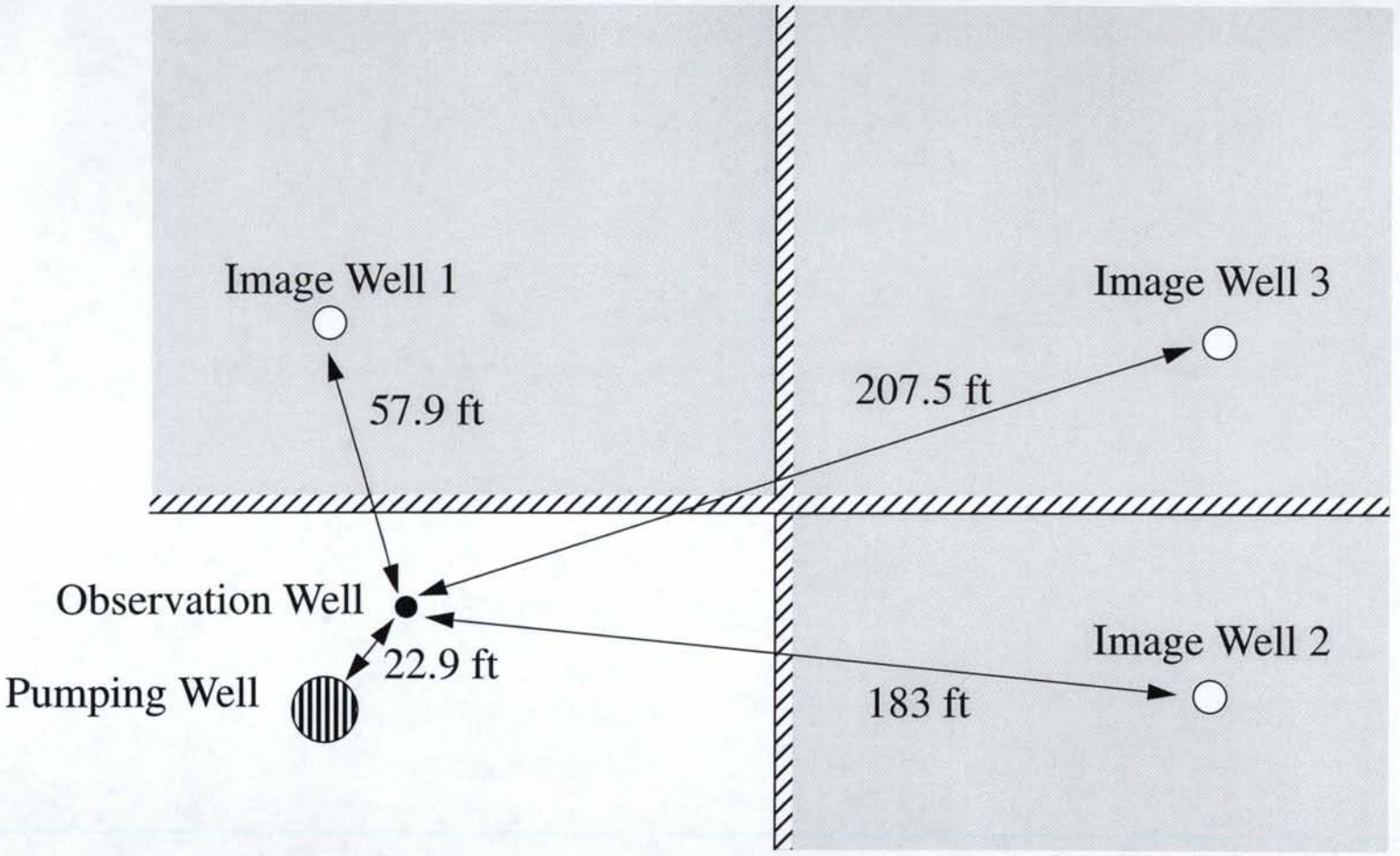

Figure A9B. Scenario 4 - Intersecting no-flow boundaries. For this scenario, Q = 30 ft^3 min^{-1}, b = 25 ft, K = .1 ft min^{-1}, and S_s = .0001 ft^{-1}. Relative positions of wells (real pumping well, observation well and image wells) and no-flow boundaries shown here were used in model with results shown in Figure A10B.

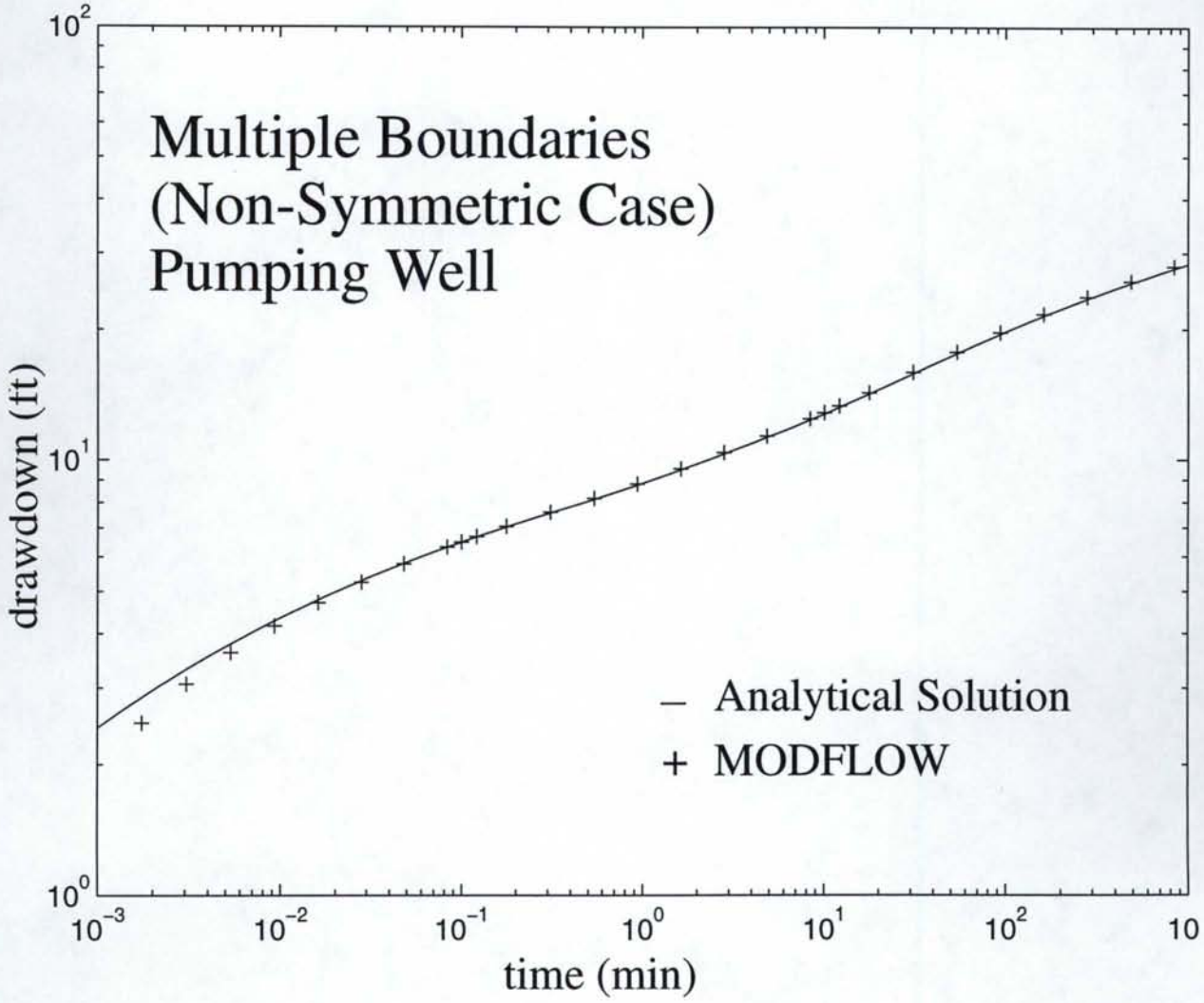

Figure A10A. Comparison of model results at the pumping well.

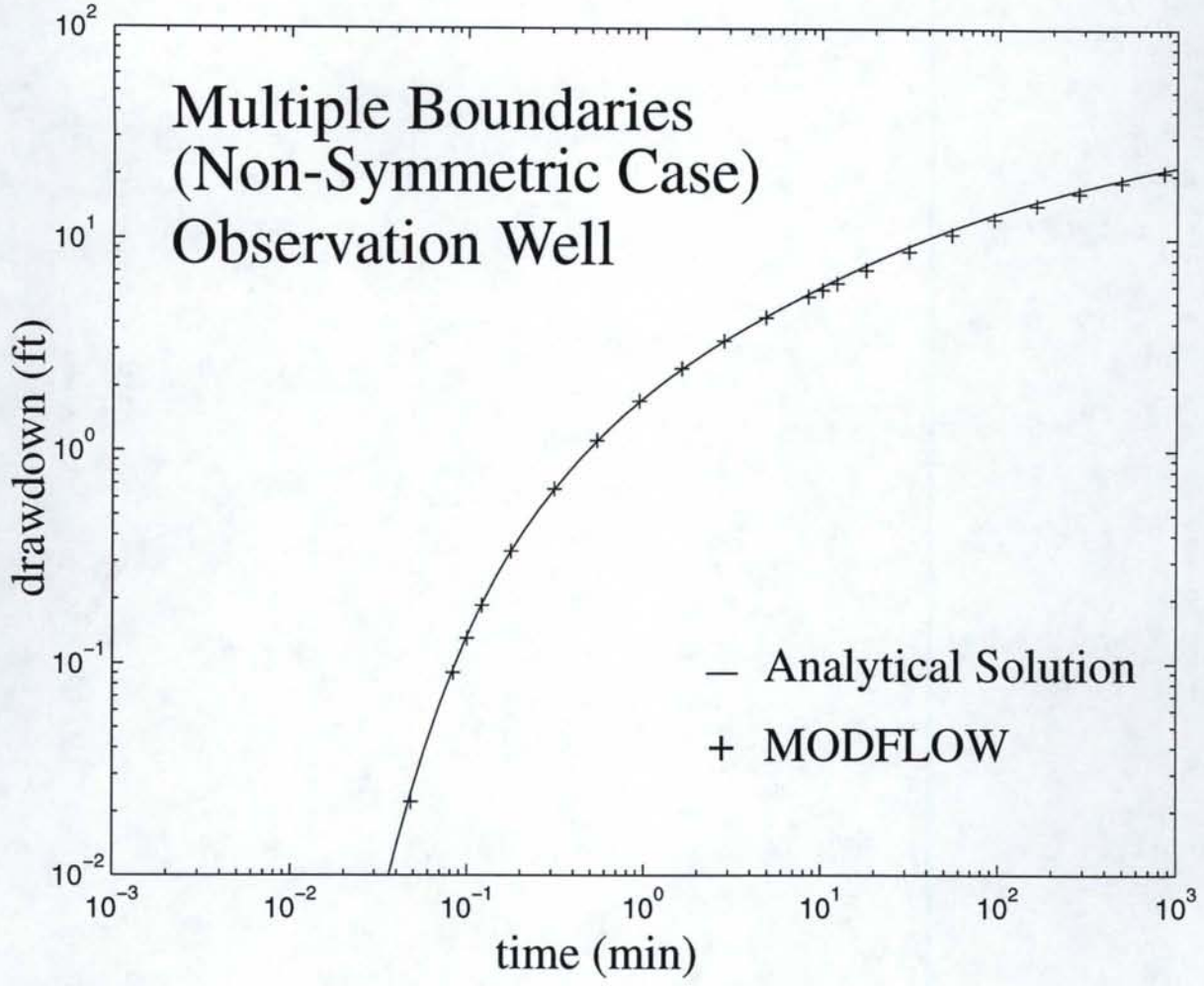

Figure A10B. Comparison of model results at an observation well.